Technical Report

TR-01-06

Analysis of groundwater flow beneath ice sheets

Boulton G S, Zatsepin S, Maillot B

University of Edinburgh
Department of Geology and Geophysics

March 2001

Svensk Kärnbränslehantering AB
Swedish Nuclear Fuel
and Waste Management Co
Box 5864
SE-102 40 Stockholm Sweden
Tel 08-459 84 00
+46 8 459 84 00
Fax 08-661 57 19
+46 8 661 57 19

Analysis of groundwater flow beneath ice sheets

Boulton G S, Zatsepin S, Maillot B

University of Edinburgh
Department of Geology and Geophysics

March 2001

Summary

The large-scale pattern of subglacial groundwater flow beneath European ice sheets was analysed in a previous report /Boulton and others, 1999/. It was based on a two-dimensional flowline model. In this report, the analysis is extended to three dimensions by exploring the interactions between groundwater and tunnel flow. A theory is developed which suggests that the large-scale geometry of the hydraulic system beneath an ice sheet is a coupled, self-organising system. In this system the pressure distribution along tunnels is a function of discharge derived from basal meltwater delivered to tunnels by groundwater flow, and the pressure along tunnels itself sets the base pressure which determines the geometry of catchments and flow towards the tunnel. The large-scale geometry of tunnel distribution is a product of the pattern of basal meltwater production and the transmissive properties of the bed. The tunnel discharge from the ice margin of the glacier, its seasonal fluctuation and the sedimentary characteristics of eskers are largely determined by the discharge of surface meltwater which penetrates to the bed in the terminal zone. The theory explains many of the characteristics of esker systems and can account for tunnel valleys. It is concluded that the large-scale hydraulic regime beneath ice sheets is largely a consequence of groundwater/tunnel flow interactions and that it is essential similar to non-glacial hydraulic regimes.

Experimental data from an Icelandic glacier, which demonstrates measured relationships between subglacial tunnel flow and groundwater flow during the transition from summer to winter seasons for a modern glacier, and which support the general conclusions of the theory is summarised in an appendix.

Innehåll

1 Introduction

In Boulton and others /1999/, general relationships between ice sheet characteristics such as geometry, extent and thermal regime, the conductive properties of the subglacial bed and the large scale organisation of groundwater flow patterns and potentials were explored through a two-dimensional, flowline model. It was concluded that subglacial groundwater catchments could be very different in extent compared with catchments in the same area during non-glacial conditions. In areas of low relief potential gradients driving flow could be very much larger than during non-glacial conditions, although in areas of high relief they could be very much smaller.

The ice sheet surface is assumed to define a limiting potential surface, on the basis that water pressures can not, in any large area or for any long period, exceed ice pressures. If low subglacial transmissivities result in water pressures being increased so that they tend to exceed the ice pressure, it is assumed that a tunnel will form at the ice/bed interface and draw down water pressures at least to the value of the limiting potential surface. The purpose of the current project is to extend theory and modelling to three dimensions by exploring the role of tunnels at the ice/bed interface in determining groundwater flow patterns and potentials during glacial periods.

2 Glaciological perspective

Melting is widespread at the base of modern glaciers including the ice sheets of Antarctica and Greenland /Hughes, 1975; Huybrechts, 1986/. Surface meltwater may also penetrate to the beds of ice sheets during the summer melt period, at least in terminal zones /Reynaud, 1989/. Surface meltwater penetration to the bed through crevasses, moulins and cavities between the glacier and the flanking valley wall is widespread in alpine valley glaciers /e.g. Hubbard and others, 1995/.

The efficiency with which meltwater drains from beneath the glacier plays, through its influence on subglacial water pressures, a fundamental role in determining rates of glacier flow, instabilities such as surges, and patterns and processes of subglacial sedimentation. Water pressure distribution depends upon the rate of discharge of meltwater into the subglacial environment and the ease of drainage though it into the proglacial environment. High rates of discharge into a poorly transmissive system produce generally high water pressures, and low rate of discharge into a highly transmissive system produce generally low water pressures. The nature of subglacial drainage pathways is thus a key issue for glaciology.

Much glaciological research over the last 20 years has therefore been concerned with this problem. Research has inevitably concentrated on relatively small valley glaciers, where parts of the drainage system can be directly observed and relationships between recharge of surface water into the system, proglacial discharge from it and consequent changes in basal water pressure can be measured. During the summer melt period, most valley glaciers appear to develop one or more major R-channels /Röthlisberger, 1972/ in which the channel arches up into the ice, but may also, if its location is stable from year to year, cut an erosional channel in the underlying bed. There is now strong evidence from many valley glaciers that water reaches these channels through a distributed drainage system which enlarges and links together the natural cavities which exist in the lee of bedrock hummocks /e.g. Lliboutry, 1968; Kamb, 1987; Willis and others, 1990/. These are cases however where the glacier flows directly over a hummocky bedrock surface /e.g. Hallet and Anderson, 1980/, possibly with a thin and sporadic sediment cover. Numerous lee-side cavities lie in close proximity to each other, and as water pressures increase during the melt period, cavities extend, excess water pressures locally lift the ice from its bed, and cavities become interconnected to produce drainage pathways which become progressively better integrated as the melt period proceeds.

Where the bed of an ice sheet is composed of materials of low transmissivity (the product of stratum hydraulic conductivity and thickness), the ice sheet´s meltwater has been inferred or observed to be discharged beneath the glacier by the following processes:

- **As a thin layer at the ice/bed interface**
  If the water pressure at any point on the glacier bed is equal to the ice overburden pressure the water will flow in a thin sheet /Weertman, 1972/. Such a sheet cannot grow in thickness, it is unstable, and excess water tends to flow towards conduits /Walder, 1982/.

- **By flow through linked cavity systems**
  Because of the topographic irregularity of those glacier beds composed of bedrock, basal water will accumulate in cavities /Lliboutry, 1968/ which grow and become

linked. Water pressure in them is a direct function of water flux whereas there is an inverse relationship in channel systems /Kamb, 1987/. A system of interconnecting topographically defined conduits can be stable, whereas large channels unrelated to topography will capture smaller ones /Röthlisberger, 1972; Shreve, 1972/.

- **By flow through "canals"**
  Walder and Fowler /1994/ have suggested that distinctive conduits, which they termed canals, will develop on a glacier bed composed of deforming sediment. They will be small, incised into the sediment and will have an ice roof. They will be parts of a dense, dispersed drainage network, akin to a braided stream system. Presumably the canal walls will continuously collapse, causing them to shift their courses. Streams will have high sediment concentrations transported at low stream velocities. Their high water pressure will counteract the tendency for the ice roof to descend into the canal and close off the canal. There will be a relationship between effective pressure (p_e) (alternative use of the effective pressure concept, which describes the pressure affecting the tunnel) and water discharge (Q) of the form:

  $$p_e = kQ^{-m}$$

  where k is a constant and m is approximately 1/3. The canals will thus tend to occur where the subglacial water potential surface is close to or coincident with the ice pressure surface, and will not draw water towards them. If they are to play an important role in draining a low permeability till, they must be ubiquitous.

- **By flow in N-channels** /Nye, 1973/
  N-channels are incised downward into the bed and lie at some angle to the direction of glacier flow. Weertman /1972/ concluded that the pressure gradient around N-channels must be asymmetric, a low pressure on the up-glacier side allowing water to enter it from that direction, and a high pressure on its down-glacier side preventing water escape across that flank.

- **By flow in R-channels** /Röthlisberger, 1972/.
  These are relatively large channels with stable, subglacial rock or sediment beds and with walls and roofs of glacier ice. Most observations of subglacial drainage, albeit near the margins of glaciers, are of R-channels. Their ice walls are prevented from closing the channel primarily because of heat generation due to turbulent water flow within it. The large water flows are able to draw down water pressures along the channel to levels well below the ice pressure. The larger the discharge in the channel, the larger can be the difference between ice pressure and water pressure because of the melting effect of large discharges on the channel wall. Because the water pressure in an R-channel is lower than the ice pressure, a "bridging effect" will produce locally enhanced loads at the ice/bed interface near to the channel, thus preventing water in a basal layer from flowing into the R-channel. A basal water layer cannot therefore be the agent whereby R-channels are recharged /Weertman, 1972/. Weertman /1972/ suggested that R-channels could be recharged from tributary N-channels if these were oblique to ice flow and intercepted water flowing down-glacier in a basal water layer. It could not flow out of N-channels on their down-glacier sides because of the stress concentration that occured there, but would be discharged into R-channels to which they were tributary.

  All the above processes represent means whereby water can be discharged from beneath the glacier into the proglacial zone, where the water pressure can be assumed to be equal to atmospheric pressure. They all operate at the ice/bed interface. As all of them involve some resistance to flow, there will be backing up of water pressure in

the proximal parts of the system and a distally directed water pressure gradient, which effectively drives the flow. The backing up of pressure in the system at the ice/bed interface will general cause flow into subglacial beds to a greater or lesser extent, depending on their permeability. This leads to a further mode of discharge /Boulton, and others, 1995a; Boulton and Caban, 1995; Boulton and others, 1999/:

- **By groundwater flow**
  Although field evidence provides a good basis for reconstruction of subglacial drainage processes and patterns beneath small valley glaciers, it is not yet possible to record or infer by observation or measurement the large scale processes and patterns of drainage which control hydraulic systems on an ice sheet-wide scale. We can however study the continental surfaces of Eurasia and North America which formed the beds of ice sheets as little as 10,000 years ago, and which have been relatively little changed since they were deglaciated. Here, systems of eskers (Figure 2-1), linear sand and gravel ridges up to 50 m in height and up to 100s of kilometres in length, form radial systems, approximately parallel to the last direction of ice movement. These systems of eskers provide evidence of former subglacial meltwater flows in R-channels /e.g. Clark and Walder, 1994/. Repetitive features of these patterns are the roughly constant esker spacings at given radial distances from the ice centres, typically spacing vary from about 10 to 50 km, see Figure 2-1. Another feature is the way in which, in a down-glacier direction, new eskers are interposed between existing ones so as to increase esker frequency, see Figure 2-1 and Figure 2-2.

Figure 2-1. *Distribution of major eskers in Scandinavia. South of the margin of the shield, very few eskers occur. It is believed that "tunnel valleys" take up the role of esker tunnels. These are deep valleys cut into the relatively soft unlithified sediments and sedimentary rocks south of the shield.*

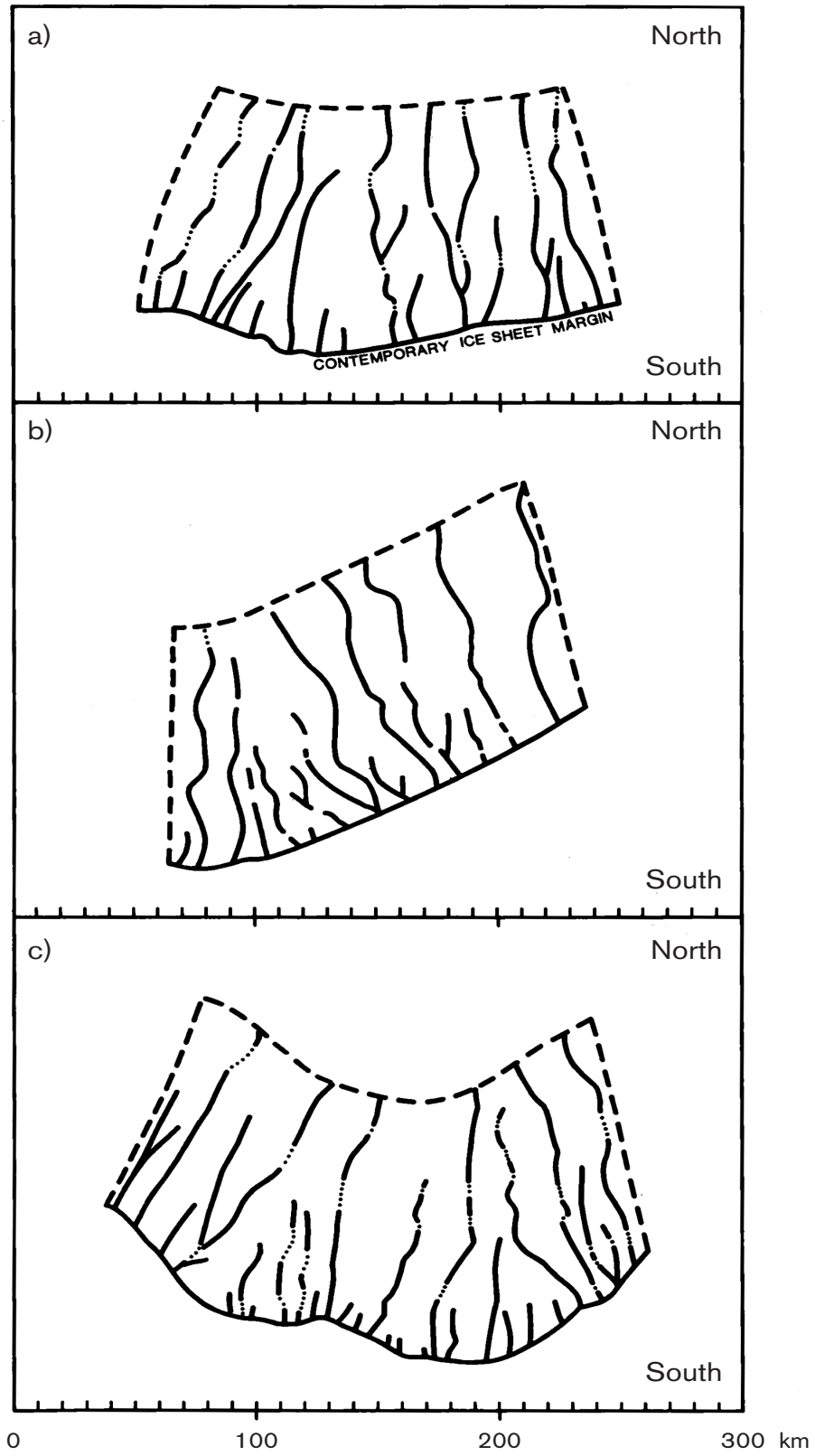

Figure 2-2. *Detailed patterns of eskers in three areas of eastern Finland. New eskers are interposed between older ones in a down-glacier direction, thereby increasing esker frequencies.*

Even in the low relief shield areas in which eskers are most frequent, bedrock tends to be covered by thick sandy tills several metres in thickness. Beds are much smoother than the predominantly rock beds of valley glaciers and there are few hummocks which might produce lee-side cavities from which distributed drainage in the sense of Kamb /1987/ might form. Any tendency for lee-side cavities would produce local deviator stresses within the bed large enough to cause collapse of the hummock /Morland and Boulton, 1975/.

Clark and Walder /1994/ have suggested that the dramatic reduction in esker frequencies which occurs at the edge of the ancient shields (Figure 2-1), reflected a change to clayey tills derived from the younger, clay-rich rocks which overlap the shields to the south. They suggested that in such areas the clay-rich bed would deform and hypothesised that conduits, which Walder and Fowler /1994/ termed canals, would form and take the place of R-channels as the primary drainage routes. Such canals would however not be the agent of distributed drainage towards R-channels on the shield.

In this report we develop a theory of large-scale drainage evolution on the bed of an ice sheet which explains the interactions between radial R-channels and water scavenged from the extensive flanking areas of melting at the base of a glacier. It is formulated on the basis of observations of subglacial drainage processes in modern glaciers and tested by its capacity to simulate and explain properties of large scale drainage systems reflected by esker distributions such as those shown in Figure 2-1. It is suggested below that groundwater flow is a key mechanism, which determines many of the attributes of the large-scale organisation of subglacial drainage systems beneath ice sheets.

3 Observations on modern glaciers

There are now many studies of time dependent subglacial water pressures measured in boreholes, which penetrate, to the beds of glaciers. Of those in which synchronous measurements have been made in several boreholes, most were made on glaciers resting on beds which were predominantly of rock /e.g. Engelhardt and others, 1978, Hantz and Lliboutry, 1983, Kamb, 1987/. In several cases, diurnal water pressure measurements at several nearby points tended to change in unison rather than show significant time lags, suggesting that interconnected cavities had been sampled.

However, an investigation by Fountain /1994/, involving a large number of boreholes penetrating to the base of the South Cascade Glacier in the USA, showed time lags of hours in the pressure responses of boreholes between which there was hydraulic connection. He interpreted this as evidence of a subglacial till layer in which Darcian flow occurred but whose low permeability caused significant time lags between different parts of the system. However, the South Cascade Glacier is a small valley glacier about 3 km in length in mountainous terrain. It is unlikely that thick permeable sediments, which may account for the apparent strong contrasts in connectivity between different boreholes, underlie the whole bed in the outer part of the glacier.

An investigation was carried on the glacier Breidamerkurjøkull in south-east Iceland, known to have a thick subglacial sediment sequence /Bogadottir and others, 1985/, to explore the pattern of subglacial groundwater flow. As the results of this experiment proved to be important in formulating the theory presented in this report, they are summarised in Appendix I.

4 Formulation of a theory of subglacial drainage beneath ice sheets and the formation of esker systems

Based on the study of modern glaciers we suggest that subglacial tunnels, which produce esker systems, are linear zones of water pressure drawdown which control the pattern of groundwater flow, the distribution of water pressures and effective pressures at the ice/bed interface. Figure 4-1 and Figure 4-2 illustrates schematically how such tunnels might be related to patterns of drawdown.

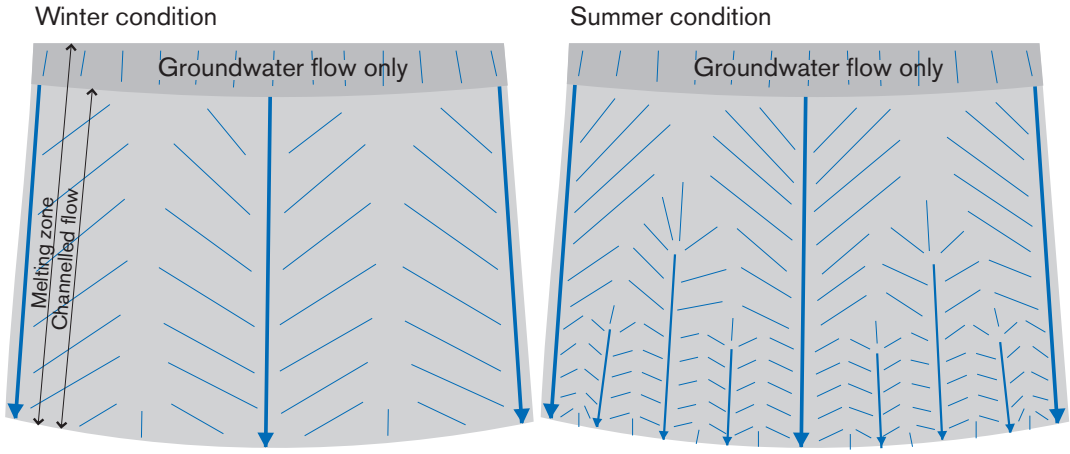

Figure 4-1. *Schematic diagram illustrating the postulated patterns of groundwater flow in relation to the distribution of subglacial tunnels.*

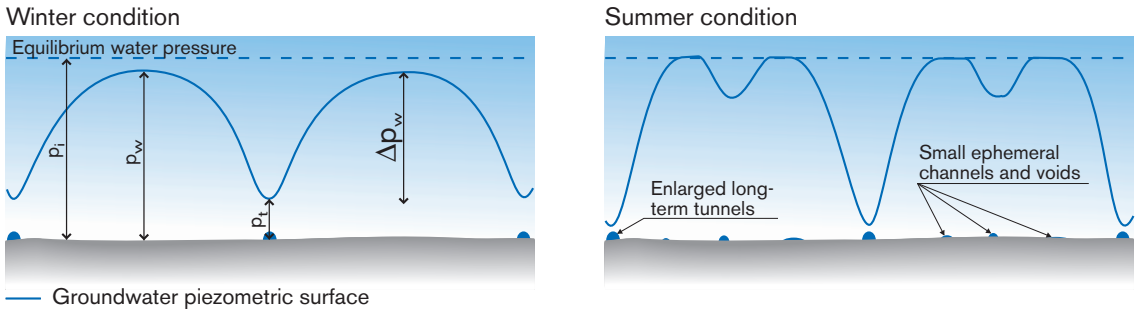

Figure 4-2 left: *Transverse cross-section of a glacier showing the postulated relationships between the groundwater piezometric surface and a subglacial tunnel during the winter period.*
right: *The situation during the summer period of high discharge. Interfluve zones of high pressure, where effective pressures tend to zero, will tend to create shortlived water filled voids. If these are able to discharge into the proglacial area pressures are drawn down and more stable tunnels are likely to form.*

The theory depends on three simple concepts:

I. Tunnels are the main agents of large-scale longitudinal meltwater discharge and groundwater flow is the mechanism whereby widespread glacial meltwater is supplied to the tunnels.

The drawdown of the piezometric surface by longitudinal tunnels ensures that groundwater flow is predominantly transverse to ice flow, thereby scavenging local meltwater for the tunnels. The tunnels themselves are the principal agents of long-distance water transport to the ice sheet margin. Existing theories which attempt show how individual drainage processes will be linked together in effective subglacial networks /e.g. Weertman, 1972/ have difficulty in explaining how water finds its way into the large R-channels which are the most efficient way of discharging large subglacial meltwater flows. The enhanced load effect in the vicinity of a tunnel either on a hard bed /Weertman, 1972/ or soft bed /Alley, 1992/ produces a effective pressure gradient away from the tunnel at the ice/bed-interface. R-channels can however be recharged efficiently by subglacial meltwater alone if they are fed through groundwater. Although a water layer at the ice/bed interface will be prevented from flowing towards an R-channel because of locally high effective pressure near the tunnel, groundwater will be drawn towards the tunnel by the lower water pressure in it. The strength of the rock skeleton will insure that interstitial pore spaces or complex fracture systems will not be closed merely because of an increase in effective pressure, although they may become smaller, leading to an increase in potential gradient in order to maintain the water discharge.

II. Tunnel spacing depends upon bed transmissivity and water recharge into the system.

Consider the transect shown in Figure 4-2 (left). If the rate of basal melting or the rate of ingress of surface meltwater were to increase, the potential gradient driving groundwater flow would produce an increase in head elevation at the groundwater divide. If this were to rise to equal or exceed the ice pressure, we would expect development of a water-filled cavity at the ice/bed interface. For reasons which will be discussed later, we anticipate that this will occur first at the glacier margin and will propagate up-glacier, thereby producing an R-channel (tunnel) which will grow in the up-glacier direction. The minimum tunnel frequency will be that which ensures that the groundwater head is everywhere below the ice head. An analogous groundwater system exists in polders in the Netherlands, where farmers dig drainage ditches with a spacing which is just small enough to draw down the water table beneath the surface at inter-ditch drainage divides. Figure 4-2a show a transverse cross-section of a glacier in which the groundwater head is drawn down by a tunnel by an amount Δp_w. As the tunnel comes nearer to the ice sheet margin, the ice pressure (p_i) begins to descend below the level of the water pressure at the groundwater drainage divide. As a consequence, a new tunnel develops and the groundwater head is drawn down on either side when $p_w \geq p_i$.

III. Winter discharges, produced entirely by basal melting, are the determinants of tunnel system and structure, and summer discharges, which include surface meltwater, which finds its way to the bed in the terminal zone, determine the maximum stream discharges and are largely responsible for esker production.

Winter and summer seasons subject most glaciers to strongly contrasting hydrological regimes. In winter, surface melting is largely absent, rainfall is slight, and as a consequence, water flowing at the base of the glacier is almost exclusively derived from basal melting where the bed of the glacier is at the melting point. Frictional heating due to movement of the glacier over its bed is the largest component. In the terminal zone of Breidamerkurjøkull in Iceland the basal meltwater due to friction is calculated as about 2 mm/day, compared with a 0.05 mm/day rate of melting from the geothermal flux. The

basal meltwater flux is a quasi-permanent feature of the basal hydrology in temperate-based glaciers and ice sheets. We suggest that it will lead to the groundwater/tunnel regime described in II above, and shown in Figure 4-2a, in which well developed tunnels whose maximum spacing is controlled by the need to ensure that $p_w < p_i$. For a basal recharge rate (m) and a bed transmissivity (T), the potential gradient towards the tunnel in the transverse (y) direction will be:

$$\frac{\partial \Delta p_w}{\partial y} = \frac{my}{T} \qquad (1)$$

As thew maximum tunnel spacing will occur when $\Delta p_w + p_t = p_i$, where p_t is the water pressure in the tunnel, the distance (L) from tunnel to drainage divide can be obtained by integrating the pressure gradient from tunnel to divide, giving:

$$\Delta p_w = \frac{m}{2T} \cdot L^2 \qquad (2)$$

So that tunnel spacing (2L) is:

$$2L = \sqrt{\frac{8T \cdot \Delta p_w}{m}} \qquad (3)$$

In the summer season, we expect surface meltwater to penetrate to the bed through crevasses and moulins in the terminal zone. It is not clear how broad this zone will be. In a slowly flowing, poorly crevassed ice sheet in which cold ice is advected into the terminal zone from a high elevation on the ice sheet summit /e.g. Boulton and Payne, 1994/, such penetration may occur in only a very narrow zone of less than 10 km extension. In more heavily crevassed ice sheets and glaciers, meltwater penetration may occur through much of the ablation area, which can extend 50–100 km from the ice margin. The rate of penetration of surface meltwater to the bed can be much larger than the basal melting rate. During days of strong melting in midsummer at Breidamerkurjøkull in Iceland, we estimate a peak recharge to the bed from this source, averaged over the whole terminal zone, of about 40 mm/day and an average midsummer recharge rate of about 15 mm/day (unpublished results). As consequence of such circumstances, water pressures will rise to the level of ice pressures at a relatively short distance from the tunnel (Figure 4-2b) and stream discharges along the tunnel will be at least 10 times larger than winter discharges. Thus we expect a seasonally oscillating flow along a tunnel. We expect water filled cavities to develop in the zone where $p_w \geq p_i$, and suggest that they may have the characteristics of canals as described by Walder and Fowler /1994/ or of features produced by hydraulic piping. Many of the water filled cavities will form locally beneath the bases of water conducting moulins and crevasses. They will not initially be interconnected, and are unlikely to develop into well integrated drainage routes by the end of the summer season. During the winter season, such drainage routes will be closed by ice flow, and as the stable bed geometry offered by a rock bed with a stable pattern of lee-side cavities is not available, the same drainage route pattern will not be re-established in the following summer. The relatively long winters and short summers characteristic of the climates around large ice sheets will militate against establishment of well integrated summer drainage route patterns. Even in warm maritime environment such as that of southern Iceland, the period of high melt rates only lasts for three months at more than 5 km from the glacier margin.

The subglacial hydraulic system described above is coupled on a large scale. Water pressure varies along a tunnel as a function of water discharge through the tunnel, but discharge is determined by the organisation of groundwater heads and catchments which are adjusted to the pressure distribution along the tunnel. We first analyse the pressure distribution along a tunnel, then the groundwater response to a given pressure distribution, and then the coupling between them.

5 The water pressure profile along a subglacial tunnel

In this section we derive the distribution of water pressure $p_t(x)$ along a subglacial tunnel, where x is the coordinate along a tunnel, as a function of the water flux Q. The analysis is based largely upon the physical analysis of Röthlisberger /1972/.

The cross-sectional area S of the tunnel at any given point is determined by the balance between the rates of melting and ice flow (tunnel closure):

$$\frac{\partial S}{\partial t} = \frac{M}{\rho_i} - 2SA\left(\frac{P}{n}\right)^n \tag{4}$$

where the effective pressure P is the difference between ice pressure p_i and pressure of water in the tunnel p_t; A and n are ice flow parameters; and ρ_i is the density of ice. The tunnel wall melting rate M depends on the water flux Q in the tunnel, (the volume flowing through the cross-sectional area S in unit time). The flow of water in the tunnel depends in part on its cross-sectional area S, and can be expressed by the empirical Manning's formula for turbulent flow in a pipe:

$$\frac{dp_t}{dx} + \rho_w g \sin\Theta = NQ^2 S^{-8/3} \tag{5}$$

where

$$N = (4\pi)^{2/3} \rho_w g m^2 \tag{6}$$

and $\rho_w g \sin\Theta$ is the component of the gravitational acceleration along the tunnel. Parameter m *in* Equation (6) is the Manning roughness coefficient /White, 1979/.

Consideration of the energy balance for steady-state flow of water in a glacier tunnel gives the tunnel wall melting rate M as a function of the water flux Q for a given water pressure profile (Paterson, 1994):

$$\left[(1-E)\frac{dp_t}{dx} + \rho_w g \sin\Theta\right] Q = ML \tag{7}$$

where L is the specific latent heat of fusion of ice and the parameter E is a combination of known physical constants describing the change in the melting point of ice due to changing water pressure along the tunnel. Elimination of the water pressure gradient from Equations (5) and (7), and assuming a horizontal tunnel, gives an equation for tunnel wall melting rate M as a function of the water flux Q and cross-sectional area S:

$$M = (1-E) N Q^3 S^{-8/3} L^{-1} \tag{8}$$

The assumption of a steady-state tunnel shape ($\delta S/\delta t = 0$) in Equation (4), with tunnel wall melting rate M given by Equation (8), results in the cross-sectional area S of the tunnel as a function of water flux and effective pressure P:

$$S = \left(\frac{(1-E)N}{2L\rho_i A'} \right)^{3/11} Q^{9/11} P^{-3n/11} \tag{9}$$

where

$$A' = A\left(\frac{1}{n} \right)^{-n} \tag{10}$$

Note, that for the ice flow parameter $n = 3$, the cross-sectional area of tunnel can be approximated as:

$$S \infty \left(\frac{Q}{P} \right) \tag{11}$$

Therefore, as a first approximation, the cross-sectional area of the tunnel with a steady-state flow of water is directly proportional to the water flux Q and is inversely proportional to the effective pressure P in the tunnel. Substitution of S in the form of (9) into the Manning's Equation (5) yields a first order non-linear differential equation for water pressure profile along the tunnel:

$$\frac{dp_t}{dx} = BQ_0^{-2/11} q(x)^{-2/11} (p_i - p_t)^{8n/11} \tag{12}$$

where B is a combination of known physical constants:

$$B = \left(\frac{2L\rho_i A'}{1-E} \right)^{8/11} N^{3/11} \tag{13}$$

and where we have introduced the dimensionless profile of the water flux:

$$q(x) = Q(x)/Q_0 \tag{14}$$

where Q_0 is a total discharge at the open end of a tunnel. An asymptotic analytical solution of Equation (12) for relatively low water pressures p_t comparable with the overburden pressure of the ice sheet is given in Appendix II.

Equation (12) is valid only for strong turbulent water flow in the tunnel with the Reynolds number $R_e = (\rho v d/\upsilon)$ greater than 2,000; where d is the tunnel diameter, υ is the characteristic velocity of water flow, and u is kinematic viscosity. At the end of the tunnel where the velocity of water flow is relatively low Equation (12) does not hold and has to be substituted with the equation for the diffusion flow of groundwater in the formation zone. Figure 5-1 shows a typical distribution of water pressure along a tunnel. There is a notable change in the water pressure profile in the region of Reynolds numbers around $R_e \cong 2{,}000$. The absolute value of water pressure in the tunnel at a given distance from the tunnel mouth depends on the value of total discharge in the tunnel. This dependence is relatively insignificant for tunnels with high total discharge, but results in an abrupt increase in water pressure for small newly created tunnels.

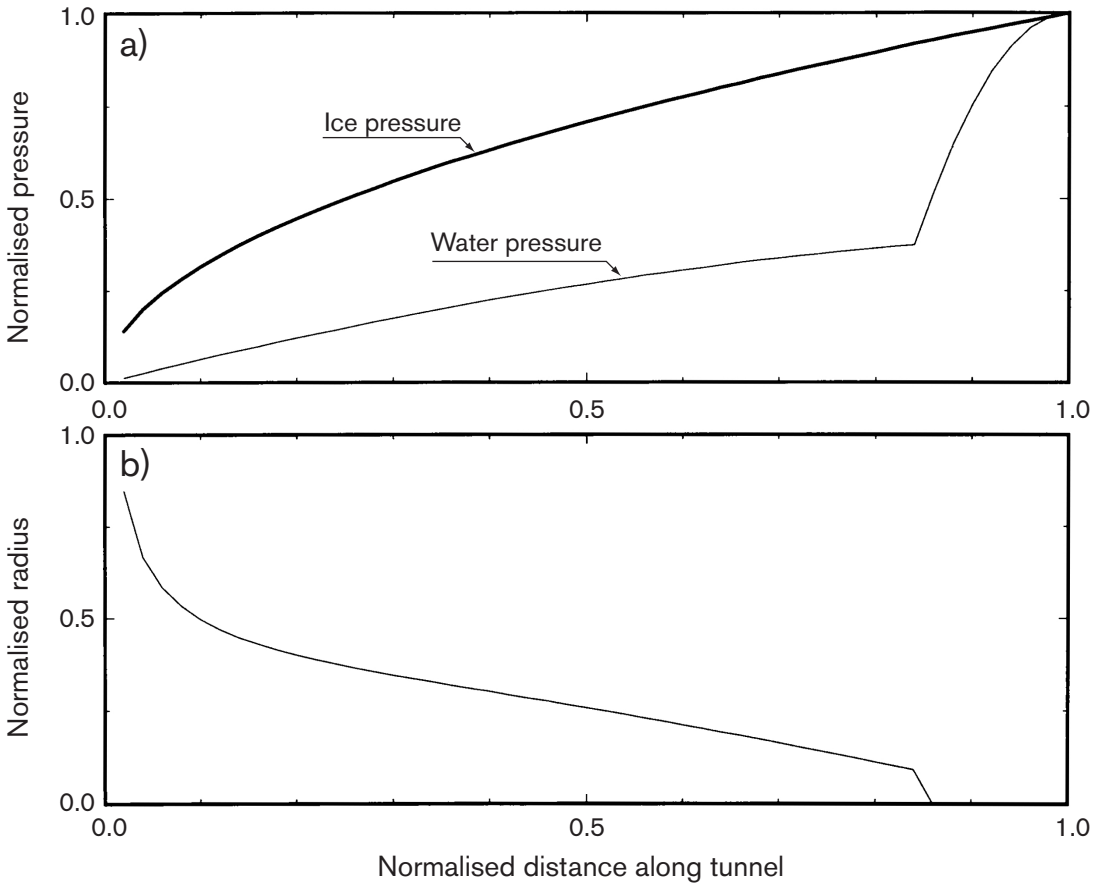

Figure 5-1. *Normalised plots showing:*
a) *The distribution of water pressure along a tunnel.*
b) *The radius of the tunnel along its length.*

It is also important to note that the weak dependence of water pressure on water discharge along the tunnel, particularly for high discharges, means that water pressure, and therefore effective pressure could be regarded, in a first approximation, as discharge independent. This result could facilitate palaeoenvironmental reconstructions based on esker distributions.

Whereas the basal meltwater component of tunnel discharge will vary only slowly, penetration through the terminal zone of the glacier of surface meltwater during summer will create seasonal cyclicity in subglacial water flow near the ice margin. Large discharges will be produced in the terminal zone during a short summer season and much lower discharges during the long winter season. This seasonal fluctuation is illustrated in Appendix I, Figure I.4 in data from Breidamerkurjøkull. The effect of the seasonal fluctuation of meltwater discharge is to change the distribution of water pressure along the tunnel such that it oscillates seasonally. However, in view of the nature of the relationship in Equation (12), the winter increase in tunnel pressure is not large.

6 The impact of tunnel formation on groundwater flow

In our theory, tunnel discharge and groundwater flow are coupled. The groundwater flux into the tunnel will depend on tunnel spacing, tunnel spacing depends upon drawdown by the tunnel and this in turn depends upon the groundwater flux into the tunnel. We first however explore the uncoupled impact of tunnel drawdown on groundwater flow.

If we consider a growing ice sheet with an outer zone of melting and an inner zone of freezing which progressively extends over permeable substratum (Figure 6-1a), the maxi-

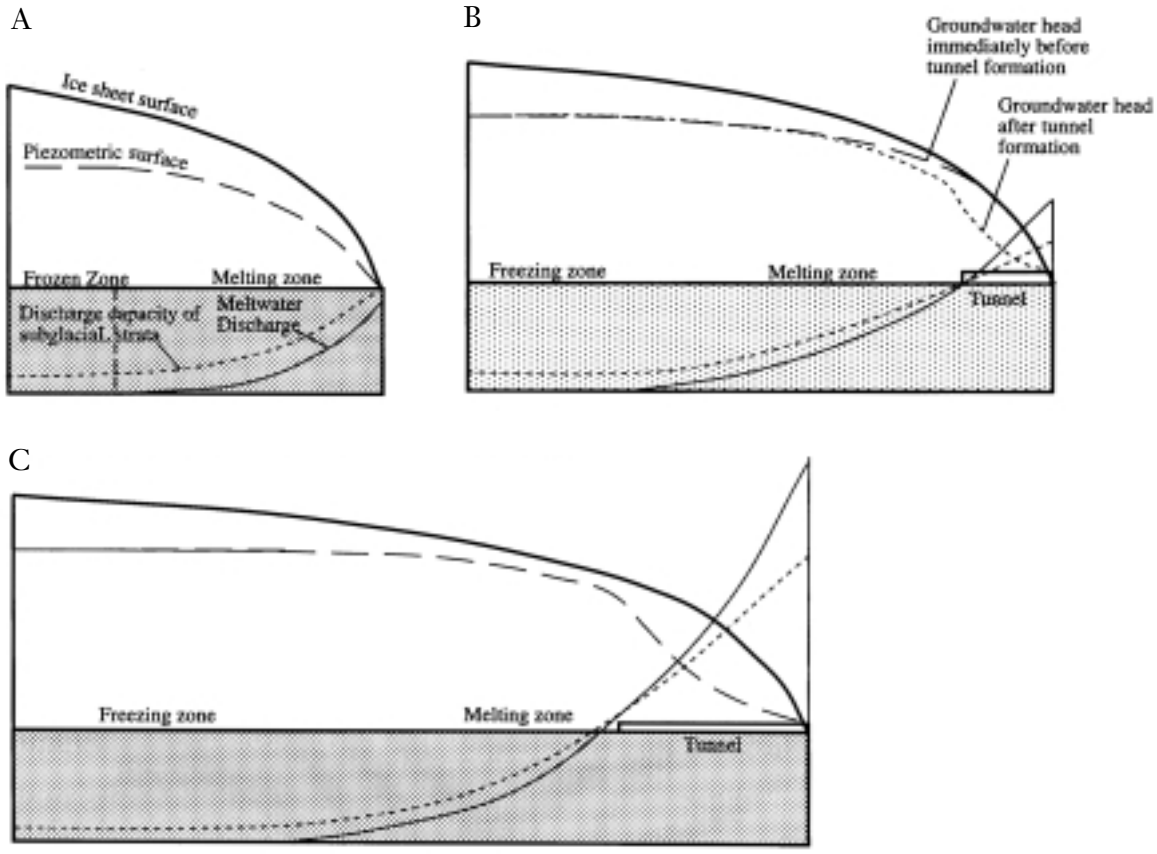

Figure 6-1. *A conceptual model of the evolution of subglacial water discharge, groundwater head and tunnel development.*
A *Small ice sheet in which the transmissivity of subglacial strata is large enough to discharge all the integrated meltwater flux.*
B *Growing ice sheet in which the integrated melt exceeds the bed transmissivity in the terminal zone of the glacier so that the water pressure builds up to the value of ice pressure, leading to tunnel formation. A consequence of this will be to draw down water pressures, although this is not shown.*
C *Further growth of the ice sheet in which the proximal end of the tunnel moves forward because of reducing discharge at the former proximal tunnel extremity (because of advance of the frozen zone). The distal end of the tunnel advances at a rate greater than the advance of the proximal end, thereby lengthening the tunnel, because the ice sheet terminus advances more rapidly than the frozen zone. The diagram shows water pressure drawdown by the tunnel.*

mum subglacial discharge of meltwater can be initially accommodated entirely by groundwater flow. As the ice sheet expands (Figure 6-1b,c), the melting zone broadens. The maximum subglacial meltwater discharge increases, the transmissivity of subglacial rocks in the terminal zone of high discharge is no longer adequate to discharge the melt flux, water pressures in the terminal zone rise to equal ice pressure, tunnels form and the water pressure is drawn down as a consequence. As soon as tunnel formation occurs, flow can no longer be treated as a two dimensional process (see Figure 4-1).

6.1 Flow in a section transverse to ice flow

We have simulated progressive groundwater drawdown due to tunnel formation in a section transverse to ice flow, which advects forward with ice flow in the terminal zone of tunnel formation. The advecting section includes a permeable rock stratum lying between the impermeable ice sheet and an impermeable basement. We use a lattice Boltzmann model to solve the diffusion equation for pore fluid pressure (Maillot and Main, 1996). The permeable stratum is a two dimensional vertical slice perpendicular to the direction of the ice flow. Its aspect ratio is 1:6.35 (i.e. its thickness is 1/6.35 times its width). The stratum is overlain by an ice sheet, which is five times thicker.

Stratum diffusivity ($D = 10^{-2}$) is isotropic and homogeneous and neither varies with time nor pressure. The fluid pressure in the stratum is normalised to the pressure of the overlying ice sheet, $p_i = \rho_i gh$, where h is ice thickness.

We initially consider a stratum in which dimensionless water pressure at the ice/bed interface is equivalent to 95% of the ice pressure, and increases linearly (hydrostatic) with depth (z):

$$p_w(y, z, t = 0) = 0.95 + \rho_w gz \qquad (15)$$

where y is distance parallel to ice flow.

The bottom boundary has a zero flux condition; the right and left boundaries match each other. At the top boundary (z = 0), a water pressure increment, which reflects pressure increase due to melting, is arbitrarily added at each time step:

$$\left(\frac{\partial p_w}{\partial t}\right)_{meltwater} = 5 * 10^{-4} \qquad (16)$$

Where and when the water pressure at z = 0 equals 1 (i.e. it equals ice pressure), it is dropped and fixed for the rest of the simulation to a random value between 0 and 1 as an arbitrary means of simulating tunnel creation. Rather than permitting water pressures to increase uniformly and therefore to produce tunnels everywhere simultaneously, we have added a random variation (of magnitude $5*10^{-4}$) to the increasing water pressure field to simulate the natural variability, which would arise from the variability of rock transmissivity.

Once a tunnel is created, we introduce an arbitrary time scale for equilibration of the pressure around the tunnel, as we do not simulate the flow of ice as in section 5, in which equilibration processes occur "naturally". During equilibration, the increase of pressure due to melting is stopped. Equilibration lasts for 1,000 time steps after tunnel creation (more than one tunnel can be created at one time). It is equivalent to the time

needed by melt production to add a normalised pressure of 0.5 at the base of the ice sheet. This artificial time scale has the spurious effect of substantially decreasing the pressure at z = 0.

Figure 6-2 shows the successive normalised water pressure heads during successive phases of tunnel creation and equilibration. The successive tunnels created are numbered. Four tunnels were created during each of events 1 and 2 and succeeding events each created one tunnel. The final profile is an approximately steady-state profile, corresponding to equilibrium between meltwater production and underground water drainage by the tunnels. Tunnels with a strong drawdown are recharged from a wide groundwater catchment, smaller drawdowns are associated with narrower catchments.

Figure 6-2 also shows the steady-state water pressure field in the subglacial permeable stratum. It shows complex bulbs of pressure drawdown. The tunnels between 15 and 80 on the horizontal scale for instance, produce a single bulb of drawdown at a depth of 18, which has split into three bulbs by a depth of 8, and 8 by a depth of 2.

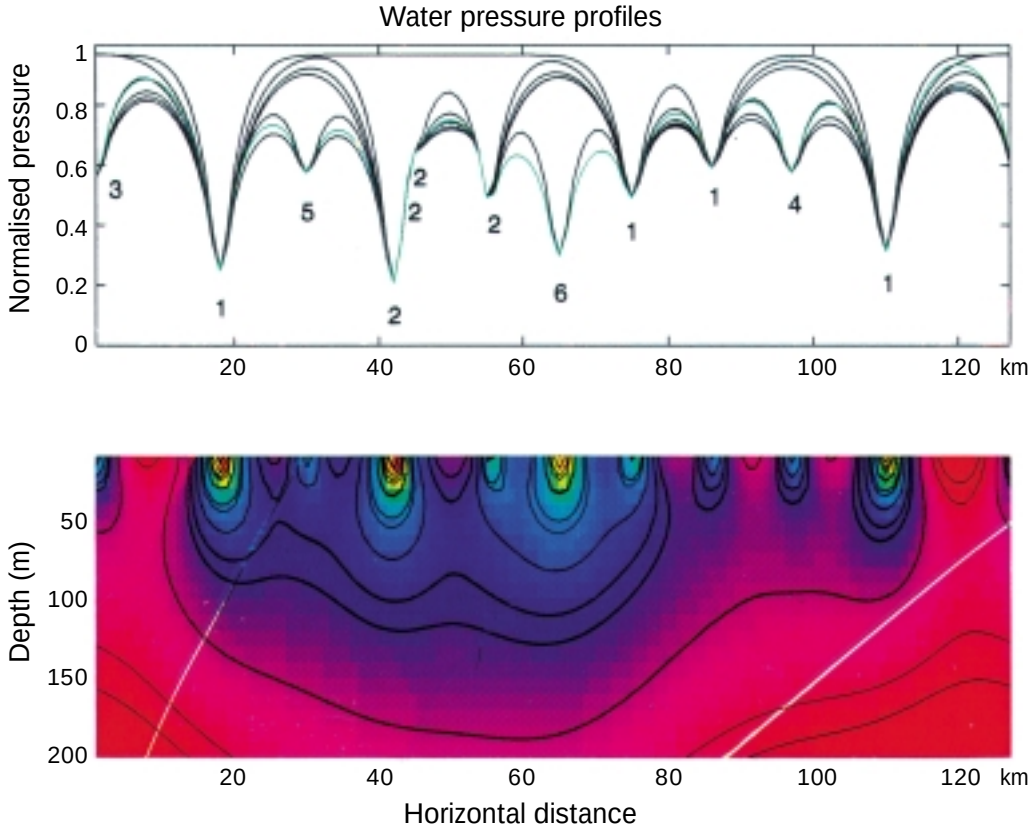

Figure 6-2. *Modelled successive water pressure heads in a subglacial stratum in a transverse cross-section, which advects towards the ice margin with the flow of the glacier. The upper diagram shows heads at the top surface of the stratum. The initial tunnels are marked 1), and successive tunnels 2), 3), 4) and 5). Tunnels marked 1) form as shown in Figure 0-1 when the water pressure in the stratum equals the ice pressure. Subsequent tunnels form as the water discharge increases through the advecting cross-section and water pressures at groundwater interfluves locally equal ice pressures. Tunnels form and rapidly draw down water pressures. The lower diagram shows heads in the subglacial stratum at the end of the tunnel forming sequence. Note the strong cones of drawdown associated with the tunnels and the way in which smaller, later tunnels are "nested" within earlier ones.*

Two dimensional, steady state water velocity profiles were calculated from Darcy's law:

$$v = -\phi\beta D(\frac{\partial p_w}{\partial x} - \rho_w g) \tag{17}$$

normalised to the velocity of the meltwater entering the ground

$$v_m = -\phi\beta D(\frac{\partial p_w}{\partial t}) \tag{18}$$

Figure 6-3 shows two-dimensional velocity vectors, expressed as square roots in order to show the velocities at depth, which would otherwise have been too small to be seen. It shows strong downwards flow into the aquifer beneath groundwater interfluves and very strong upward flow into tunnels. The zones of upward flow converge towards the tunnels.

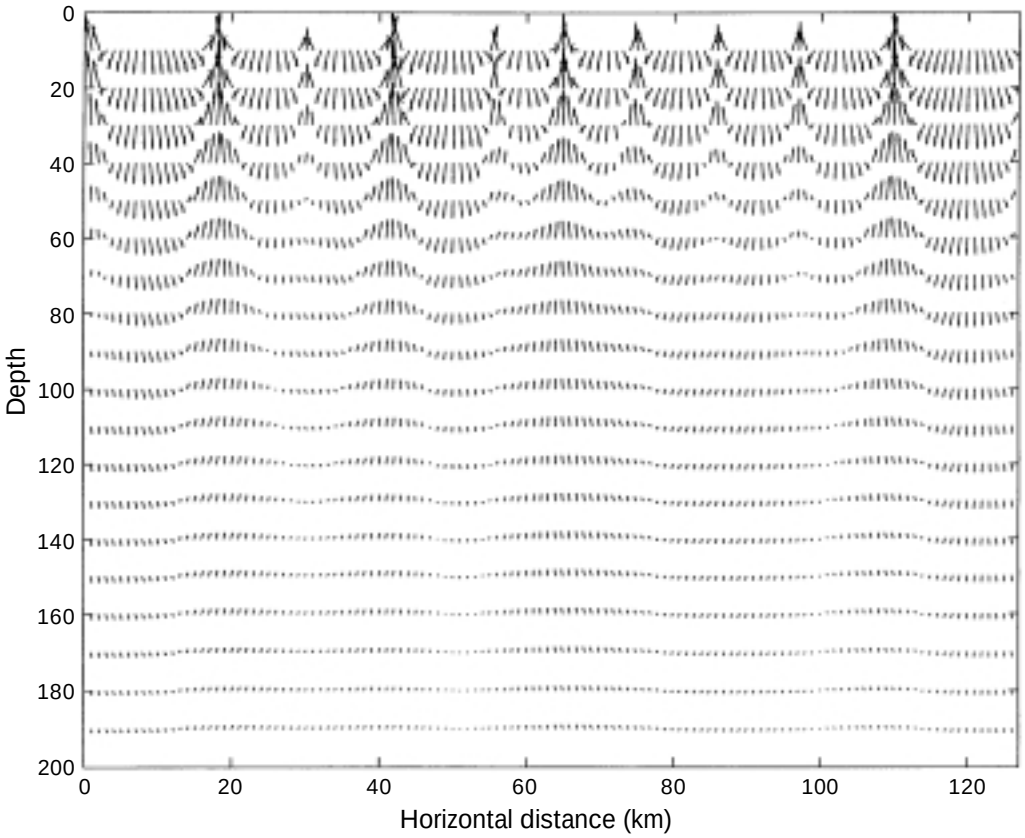

Figure 6-3. *Groundwater velocity vectors (explained as square roots in order to show velocities at depth) for the lower diagram of Figure 6-2.*

6.2 Evolution of drainage systems through a glacial cycle

We now wish to explore the evolutionary pattern of drainage systems on the bed of an ice sheet flowing over a horizontal bed through the whole of a glacial cycle of growth and decay.

Boulton and Payne /1994/ have simulated the thermal evolution of the European ice sheet through the last glacial cycle, and suggested that patterns of basal thermal regime in time and space are likely to be similar to the pattern shown in Figure 6-4. In such a pattern, we would expect several hydraulic zones to occur:

a) An inner zone of basal freezing where there is little groundwater flow and no basal tunnels.

b) A zone of basal melting where the maximum subglacial meltwater flux is sufficiently small to be discharged entirely by groundwater flow.

c) A zone where the meltwater flux is too large to be discharged by groundwater flow alone, and in which tunnels form, draw down heads and influence groundwater flow in the way described in the previous sections. Tunnel discharges would remain relatively small.

d) An outer zone in which surface meltwater is able to penetrate to the bed during summer thereby creating large summer discharges capable of generating large eskers composed of relatively coarse grained materials.

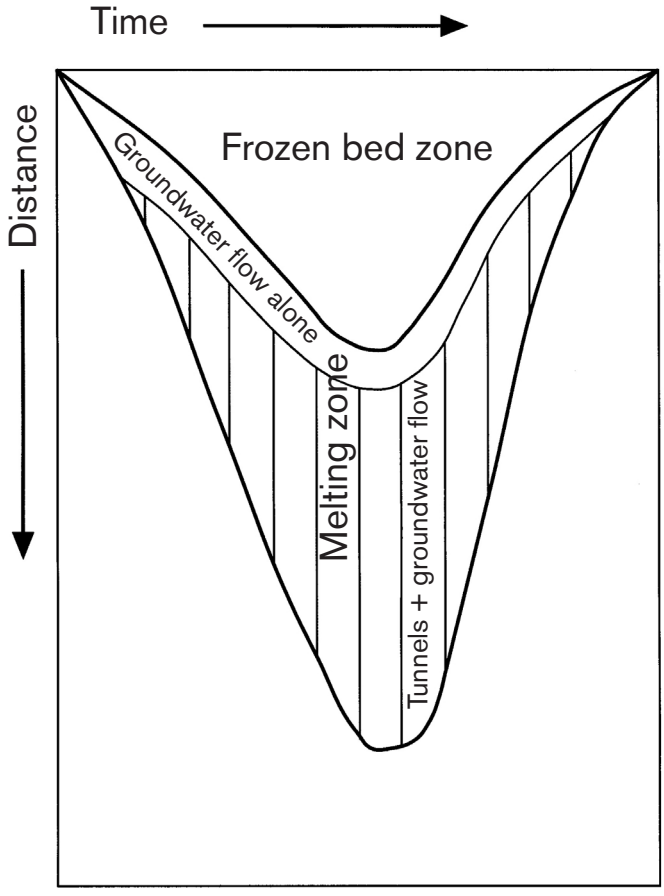

Figure 6-4. *Generalised pattern of basal thermal regimes and associated hydraulic regimes beneath an ice sheet during a complete glacial cycle.*

We have simulated the pattern of meltwater tunnels and associated groundwater flow, which would be produced during such a glacial cycle. A pattern of time dependent ice sheet change was prescribed based on the models produced by Boulton and Payne /1994/ , but in which ice sheet form and basal melting rate are reduced to a simple form. We have assumed, as concluded above, that the pattern of large, well-integrated meltwater tunnels is likely to be determined by the long-term patterns of basal melting and that the short summer season has a brief and impersistent impact on the tunnel system. It does however play the dominant role in sediment production, as summer discharges, enhanced by surface meltwater penetrating to the bed in the terminal zone, are far in excess of winter discharges.

We have modelled a time-symmetrical 20,000 years long glacial cycle during which the ice sheet expands from its initiating core to its maximum extent and retreats again. The rate of basal melting, believed to be the long-term determinant of the drainage system, increases monotonically from zero at the ice divide to a maximum of 63.5 mm per year at the ice margin (based on Boulton and Payne /1994/). Ground diffusivity is set to 10^{-2} m^2s^{-1}. The topography of the ice sheet surface is derived from Boulton and Payne /1994/.

As the ice sheet expands, and the meltwater discharge at the ice margin increases, a point is reached where meltwater can no longer be discharged by groundwater flow alone (Figure 6-1), and groundwater pressures tend to exceed ice pressures. At this point, a tunnel will form in the terminal zone and will lengthen as the ice sheet expands. This first, reference tunnel is created at an arbitrary point ($p_{t1}(z)$). Where z is a dimensional coordinate ($z = (x/x_t)$), where x_t is the length of the tunnel. For all subsequent tunnels:

$$p_t(z) = p_{t1}(z=1)\left(\frac{x_t}{x_{t1}}\right)^{2-4/11}\frac{180}{121}f(z) \tag{19}$$

$$f(z) = \frac{121}{180} - \frac{11}{180}(1-z)^{\frac{9}{11}}(11-9z) \tag{20}$$

where we assume that $Q_0 \propto x_t^2$, where Q_0 is the discharge at the open end of the tunnel, and defines $p_{t1}(z=1)\beta$, p_i(z=1 of reference tunnel).

In the simulation, we put $\beta = 0.8$. A tunnel is created when $p_w > p_i$. Normalisation is carried out in relation to the maximum ice pressure at the maximum extent of the ice sheet:

$$p_t \rightarrow \tilde{p}_t = \frac{p_t}{p_{t,\max}} \tag{21}$$

$$p_i \rightarrow \tilde{p}_i = \frac{p_i}{p_{i,\max}} \tag{22}$$

Results of a simulation are shown in Figure 6-5, illustrating the evolution of the system during the growth phase of the ice sheet. Using transmissivities for bedrock such as those suggested by Bengtsson /1997/ and melting rates suggested by Boulton and Payne /1994/ the model predicts esker spacing of the order 5–50 km when applied to esker systems in south eastern Sweden, at a distance of some 500 km from the ice divide. It represents a reasonable fit to observed spacing (Figure 6-2).

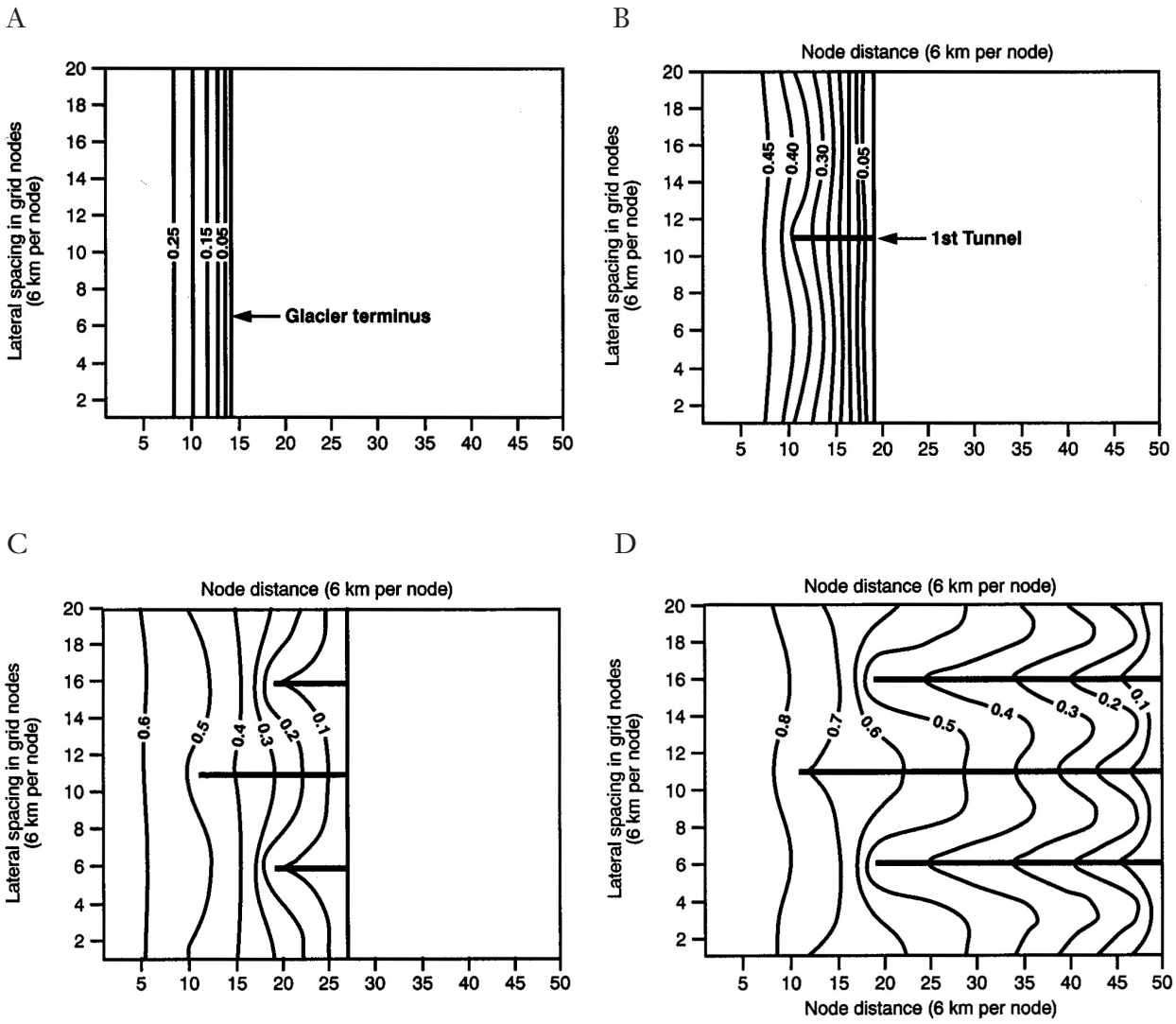

Figure 6-5. *Simulated evolution in plan of a system of basal tunnels and the associated groundwater heads.*

As a principal determinant of esker spacing is bed transmissivity, we suggest that esker spacings could be thought of as providing a measure of the large-scale transmissivity of the bed. In this regard, there is one feature of esker systems that the simulation based on the theory does not explain. As shown in Figure 2-2, eskers do, in some places, show downstream confluences. Initial investigations suggest that this can arise from transmissivity heterogeneity and that it could provide a further index of large-scale bed properties. We expect to explore this phenomenon at a later stage.

7 Comparison of the results with distribution of eskers formed beneath former ice sheets

We can only speculate about drainage systems beneath the modern ice sheets of Greenland and Antarctica. The surfaces over which ice sheets have waxed and waned during the climatic cycles of the late Quaternary in Eurasia and North America bear though evidence of subglacial drainage patterns in their widely occurring esker systems. As the theory developed above should also account for the distribution of eskers, the patterns of eskers on these surfaces should be compatible with the theory.

Figure 2-1 shows the distribution of eskers on the crystalline Scandinavian shield area of Europe produced during the last, late Weichselian decay of the ice sheet. They exhibit a radial pattern in which individual eskers lie parallel to the contemporary direction of ice flow during decay and are presumed to have formed approximately parallel to the contemporary surface slope of the ice sheet. Figure 2-2 shows detailed patterns of esker distribution in three areas of Europe. New eskers appear to be inserted in a down-flow direction. At no point do they appear to terminate in a down-flow direction, but they do occasionally show down-ice confluence. Their sedimentary structures show that most eskers are formed at or near to ice margins /De Geer, 1897, Woodworth, 1899/. They are either formed subglacially where they have blocked subglacial stream tunnels, or at terrestrial ice margins where they have been deposited as ice-contact fans at the points of proglacial discharge of major subglacial streams. They can also be formed at subaquatic margins where they have been deposited as fans at the point of discharge of major subglacial streams draining into the sea or into proglacial lakes. They may be relatively continuous ridges or series of hummocks, depending on the precise characteristics of the depositional environment.

Measurements have been made of the frequency of eskers along broad swathes parallel to average directions of ice sheet flow during the phase of deglaciation. If we restrict ourselves to the areas of crystalline bedrock in the core of the ice sheet, we find that esker frequencies increase systematically with distance from the centres of ice sheet flow (Figure 2-1) before diminishing dramatically just beyond the edge of the shield where this gives way to a fringing zone of younger, softer sedimentary rocks.

Esker ridges are not restricted however to the large-scale systems shown in Figures 1 and 2. For example, Lundquist /personal communication, 1996/ has demonstrated how, in parts of southern Sweden, relatively small, discontinuous esker fragments occur between major esker systems which do not show the continuity of those illustrated in Figure 2-1. Restricting ourselves initially to the eskers on the shield, we suggest the following:

a) Major esker systems such as those shown in Figure 1 reflect the locations of well integrated subglacial tunnels, whose spacing is primarily determined by their capacity to draw down groundwater heads in the inter-tunnel zones below the value of ice pressure. The systems are adjusted to the relatively long-term base flow component of meltwater discharge derived from basal melting.

b) The theory suggests that the spacing of large-scale esker systems (Figure 1) is a reflection of the basal melting rate and the large-scale transmissivity of the bed. The pattern of spacing of eskers in the down-ice direction expected by the theory using a constant value of bed transmissivity matches well with the patterns measured from the Scandinavian shield area. This is surprising given the variability of shield geology, from which one might presume a highly variable pattern of transmissivity, which, in turn, would lead to relatively complex patterns of spacing. It may however be that the relatively orderly pattern of spacing on the shield, is a good measure of very large-scale transmissivity, and suggests that the relatively simple pattern of large scale permeability variation suggested by Bengtsson /1997/ is realistic. There is good agreement between measured spacing and those expected by the theory when using the suggested conductivity values.

c) Surface meltwater penetrates to the base of the ice sheet in the terminal zone during a relatively short summer season. It has relatively little impact on the spacing of major esker systems, but it does contribute the dominant component to summer discharges, and is responsible for much of the mass of eskers. We suggest that evidence of cyclic sedimentation associated with eskers reflects this seaonality.

d) Relatively small, poorly integrated eskers showing little longitudinal continuity occur between major eskers. It is suggested that these are formed during summer in the terminal zone of the ice sheet, when surface meltwater is able to penetrate to the bed. Locally, and temporarily, this drives up basal water pressures to the level of ice pressures in the vicinity of moulins and crevasses, which penetrate to the bed, so that water filled cavities form. They may be analogous to the canals of Walder and Fowler /1994/. Some may produce piping, and may drain to the margin, thereby drawing down water pressures and permitting rapid, turbulent flow along the these drainage paths, thus transporting sediment and forming eskers. They are unlikely to re-form in the same place during the following year, and thus do not form part of larger, integrated esker system.

e) The theory does not, as yet, account for the branching of esker systems. We have suggested above that this is most likely to reflect heterogeneity of bed transmissivity, and this will be addressed in a subsequent development of this work.

8 Glacial palaeohydrology inferred from esker systems in Europe

The esker maps in Figure 2-2 are believed to show approximately contemporary tunnels beneath the ice sheet during its retreat, when the margin lay in the positions shown. We wish to examine whether the patterns are compatible with the theory and if so, the states of subglacial hydraulic organisation which they reflect.

We have analysed the esker pattern shown in Figure 2-2a, which we suggest reflects tunnel distribution at 10,300 years BP in part of eastern Finland. We seek a steady groundwater pressure field, which reflects equilibrium between meltwater production and its ultimate discharge through tunnels to the ice margin. From a given distribution of melting rate we determine the rate at which water must be discharged through the tunnel system shown in Figure 2a. If we estimate the discharge along an individual tunnel and know the ice pressure, we can estimate the pressure distribution along the tunnel (Equation 7). From this and the transmissivity of bedrock, we can reconstruct the groundwater pressure field. The analysis shows that the pressure field depends upon ratio of melt rate to transmissivity rather than their actual magnitudes.

The water pressure in a tunnel is derived analytically in Appendix II. It can be described in terms of a reference tunnel with water pressure profile obeyed to the non-linear differential equation:

$$p_t(z) = p_{t1}(z=1)\left(\frac{x_t}{x_{t1}}\right)^{2-6/11}\left(1-\frac{11}{121}(1-z)^{9/11}(11-9z)\right) \qquad (23)$$

where p_{t1} is the water pressure at the proximal extremity (z = 1) of the reference tunnel, x_{t1} is its length, and where we assume that the total discharge from the distal extremity of a tunnel of length x_t is proportional to the volume of rock drained by it.

The ice pressure at the base of an ice sheet is normalised to the maximum pressure within the map area, to give:

$$p_i = \left(\frac{s}{s_{max}}\right)^{1/2} \qquad (24)$$

where s is the distance to the ice margin, and s_{max} the maximum longitudinal distance to the ice margin within the map area. Water pressures within tunnels are then linked to the ice pressure by choosing:

$$p_{t1}(z=1) = \tfrac{2}{3}\, p_i \qquad (25)$$

where the ice pressure at the base of an ice sheet whose profile is normalised to the maximum pressure within the map area. All other dimensionless tunnel pressures then follow from Equation (23).

Melting rates and thermal regimes are derived from those presented in Boulton and Payne /1994/. The whole of the map area lies within the melting zone, with melting rates increasing exponentially by a factor of four from north to south across the map area.

The esker map (Figure 2-2a) was digitised and discretised on a square grid of 141 x 219 nodes in order to maintain the aspect ratio and to ensure at least two nodes between any two tunnels. Conditions at the left and right boundaries are cyclic, which does not influence the results anywhere between the leftmost and rightmost tunnels. The pressure at the up-stream boundary was maintained at an initial value defined below, and maintained at zero at and beyond the ice sheet margin. The conductive properties of the bed are assumed to be similar to those of similar Archaean basement rocks in southern Sweden. Their permeabilities are relatively high and tend to be restricted to the topmost 100–200 m. As the permeable layer has a depth which is negligible compared with the horizontal extent of the modelled area (a ratio of ca 1:1,000) and we are primarily concerned with horizontal groundwater flow, we are justified in using a 2D rather than 3D grid.

The initial pressure field is extrapolated in time according to the diffusion equation:

$$\frac{\partial p_w(x,t)}{\partial t} = D\frac{\partial^2 p_w(x,t)}{\partial x_i \partial x_j} + \left(\frac{\partial p_w}{\partial t}\right)_{meltwater} \tag{26}$$

where x represents the lattice node, and D the diffusivity of the permeable layer. The diffusivity, proportional to permeability, is chosen so that the steady-state water pressure is everywhere below the ice pressure. The pressure is extrapolated in time until a steady state is reached, when:

$$\frac{\partial^2 p_w(x,t)}{\partial x_i \partial x_j} = \frac{1}{D}\left(\frac{\partial p_w}{\partial t}\right)_{meltwater} \tag{27}$$

This latter demonstrates that the steady-state water pressure is only dependent on the ratio of melt rate to diffusivity and not to their magnitudes. Furthermore, changing this ratio would only multiply the pressure field by a constant, leaving the pattern of meltwater flow unchanged unless water pressures locally exceeded ice pressures resulting in the formation of a new tunnel, which would change the pattern of flow.

Figure 8-1 shows the resultant groundwater pressure surface for the esker pattern in Figure 2-2a and Figure 8-2 shows horizontal groundwater velocity vectors. There are several important conclusions:

a) A stable groundwater configuration is largely compatible with observed patterns of esker distribution using the theory developed in this paper.

b) Groundwater flow is dominated by transverse flow towards tunnels. In places, this even shows an up-glacier component (e.g. at coordinates 80, 50). Reconstructions of subglacial groundwater flow in the horizontal plane in which the hydraulic effect of drawdown along subglacial tunnels is not taken into account /e.g. Piotrowski, 1994, van Weert and Leijnse, 1996/ are erroneous, as are two dimensional flow-line reconstructions, which cannot simulate the effect of tunnels /Boulton and others, 1995a/.

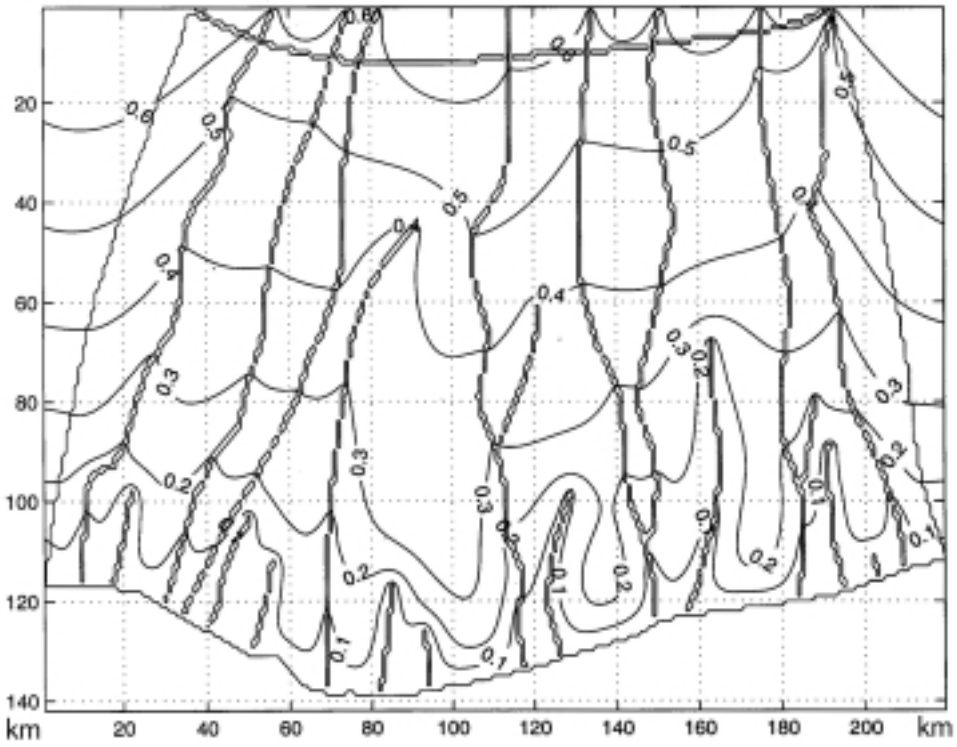

Figure 8-1. *Reconstructed groundwater heads at the ground surface for the esker pattern shown in Figure 2-2a. The lines at left, right and top of the diagram show the extent of the reliably modelled area.*

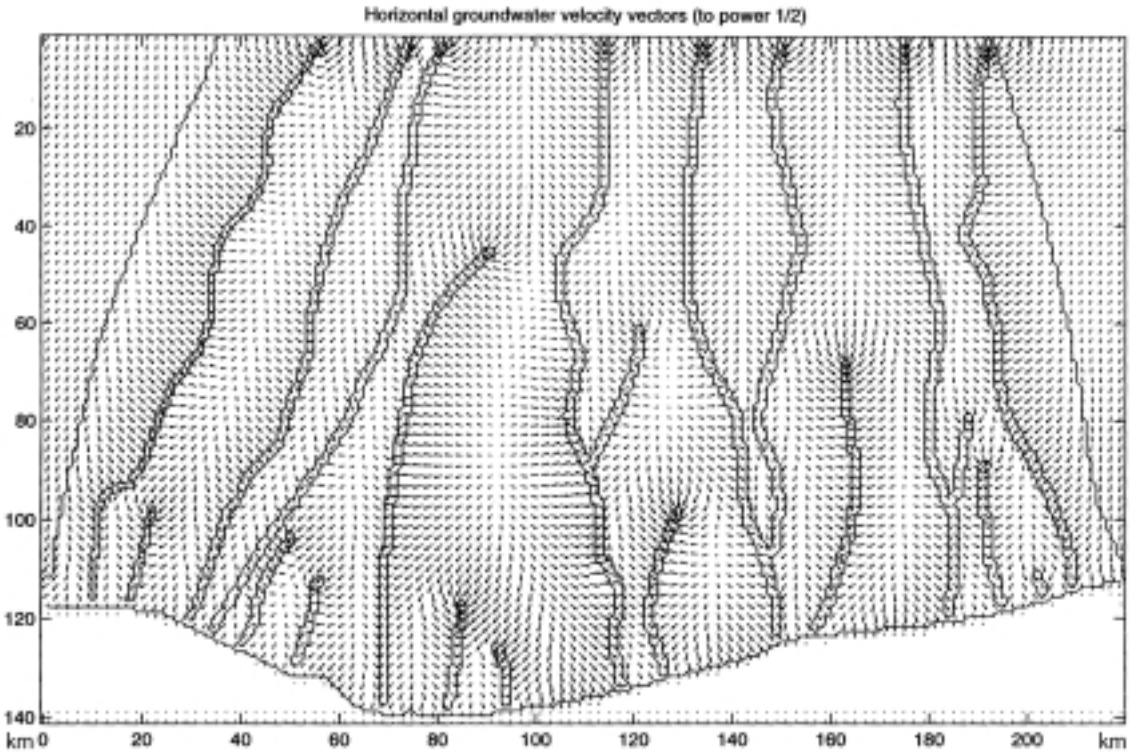

Figure 8-2. *Reconstructed horizontal groundwater flow vectors at the ground surface for the esker pattern shown in Figure 2-2a.*

c) The patterns are indistinguishable from those which are characteristic of the groundwater table and its relationship to stream valleys in unglaciated temperate regions, producing the striking conclusion of an essential similarity between the geometry of non-glacial and glaciated hydraulic systems.

d) In several places (45, 105; 70, 60; 115, 120; 180, 85; 185, 110; in Figure 8-2), short tunnels with a lower water pressure exert such a strong drawdown effect, that the gradient towards them extends across nearby larger tunnels, whose waters will therefore be captured by the smaller tunnel.

e) If closely spaced tunnels are unstable, why do they occur? In our simulation, we have assumed constant bed transmissivity. A realistic bed shows complex spatial patterns of transmissivity. If an ice margin advances over a local patch of low transmissivity, water pressures will rapidly rise to the value of the ice pressure at the margin and a tunnel will form there. As the ice sheet expands and tunnels grow down ice, the water capture referred to in d) will occur, the longer tunnel will be abandoned and its water will flow down the new distal section. An esker will form in the abandoned section, and ultimately, on ice sheet retreat, an esker will form in the newer section, producing an apparent downstream branching of eskers. Although this is not shown in the modelled example, it is shown in some of the esker systems in Figure 0-1, in northern Finland for example.

f) Figure 8-1 shows that water pressures are closest to ice pressures near to the ice sheet margin, confirming that tunnels will tend to be initiated in this zone. However, this conclusion is only valid if the basal melting rate rises towards the ice sheet margin. In the case of Breidamerkurjökull for example, the maximum basal melting rate is calculated to occur about 8–10 km from the margin (unpublished results). If tunnels are formed at such a distance from an ice sheet margin because of the increase of groundwater pressures to the value of the ice pressures, we might expect subglacial water pools to develop which we would expect to be unstable unless they lie in enclosed hollows. In time they might extend to the margin to form tunnels which will draw down water pressures and discharged large water and sediment fluxes. However, if we consider the probability that summer melting will generate a larger number of short lived tunnels at the ice margin, such summer perturbations will generate a large tunnel population from which long term tunnels can be selected in the zones of lowest effective pressure shown in Figure 8-1.

g) Shreve /1972/ developed a theory of water flow through glaciers in which the potential distribution was related to the flux of water through the ice and which assumed "water pressure in subglacial tunnels beneath the interior of ice sheets very nearly equals the glacioisostatic pressure of the surrounding ice" /Shreve, 1985/. Shreve /1985/ used this theory to reconstruct the form of an ice sheet surface profile from the trajectory over the topography of a large esker, the Katahdin esker, in Maine, USA. We suggest that the drawdown of water pressure along a subglacial tunnel is much larger than estimated by Shreve (c.f. Figure 5-1), that the self-organisation of discharge is the primary control and that potential distributions on the bed of a glacier as shown in Figure 8-1 set base pressures to which any englacial water potentials must adjust, rather than the englacial potentials determining potentials at the ice/bed interface.

9 The origin of tunnel valleys

On the softer sedimentary rocks beyond the margin of the Scandinavian shield, eskers become very rare. A similar pattern is found in North America /Clark and Walder, 1994/ where high esker densities on the Precambrian shield contrast with rare occurrences on the surrounding younger, softer sedimentary rocks. Within these latter areas, Boulton and Hindmarsh /1987/ have suggested that the role of esker-forming tunnels in longitudinal transmission of the largest part of the subglacial meltwater flux has been taken over by "tunnel valleys". These are wide (2–5 km), deep (50–400 m), relatively steep sided valleys, which often have an irregular long profile /Praeg, 1996/, which are radial to the ice sheet and for which there is as yet no entirely satisfactory explanation. They present a major unsolved problem in glacial hydrology.

Boulton and Hindmarsh /1987/ suggested that in areas of soft permeable sediments, groundwater flow controlled the spacing of subglacial tunnels and that subglacial sediment deformation under low effective pressures caused sediment flow towards the tunnels. Stream flow along the tunnels would remove sediment flowing into it. The joint operation of these two processes would cause general lowering of the bed in the vicinity of the tunnel leading to formation of a broad, deep tunnel valley.

Analysis of groundwater flow towards a tunnel (Figure 6-2) shows high values of potential gradients and groundwater flow velocities near to the tunnel. We also expect a bulb of low pressure in a shallow zone beneath the tunnel (Figure 6-2). Under such conditions of high potential gradient, high flow rates and low effective pressure, we expect fluidisation of unlithified materials to occur, where seepage pressure balances the effective pressure, and hydrofracturing of lithified materials /Boulton and Caban, 1995/. The existence of such loose materials on the bed of a tunnel will facilitate high values of transport and erosion on the bed of the tunnel, with the potential for considerable overdeepening.

Where there is a strong, lithified substratum, as in a shield area, some hydrofracturing would be expected although the gross erosion rate is unlikely to be large. There are several examples of eskers in shield areas where the esker can be shown to lie in a shallow bedrock depression trending parallel to the line of the esker and extending laterally for a short distance on both sides. We suggest that this may be a consequence of hydrofracturing of the type described above. We might also expect relatively high values of bedrock permeability beneath the esker as a consequence of hydrofracturing.

Where the substratum is much weaker as it is in the area to the south of the Scandinavian shield in Europe. The rates of erosion due to hydrofracturing and fluvial transport could be very much larger, whilst the impact of sub-tunnel liquifaction could be dramatic in helping to produce deep tunnel valleys. Tunnel valley width would depend upon the extent to which tunnel location shifted through time.

Piotrowski /1994/ has modelled the small scale pattern of subglacial groundwater flow along the line of a tunnel valley in north Germany. However, his analysis completely ignores the effect of a major stream flowing along the line of the tunnel valley in drawing down water pressures. As a consequence, Piotrowski's reconstruction of groundwater flow vectors and potentials shows them to be parallel to the axis of the tunnel valley, whereas they would have been normal to the axis.

10 General conclusions

1. Groundwater flow plays a key role in organising the large scale, continent wide behaviour of the hydraulic system beneath ice sheets.

2. The relationship between subglacial groundwater and tunnel flow is essentially similar to groundwater and stream relationships in unglaciated terrains.

3. The system is a large-scale self-organising system, which reflects and indirectly measures the large scale transmissive properties of the rocks over which the ice sheet flows.

4. The distribution of eskers and tunnel valleys in formerly glaciated regions is a reflection of the large pattern of time dependent organisation of the system.

5. The large-scale pattern of subglacial melting, which does not vary seasonally, is the principal determinant of the large-scale geometry of the system. Surface meltwater, which penetrates to the bed in the marginal zone during summer, largely determines the magnitude of tunnel discharge in summer and the sedimentological characteristics of eskers.

References

Alley R B, 1992. How can low-pressure channels and deforming tills coexist subglacially. J Glaciol, 38(128), 200–207.

Bengtsson L I, 1997. Hydraulisk konduktivitet i kristallin berggrund: Analys av djupvariation i sex svenska områden.
Chalmers Tekniska Högskola, Geologiska Institutionen Publ B446, Göteborg

Bogadottir H, Boulton G S, Tomasson H, Thors K, 1985. The structure of the sediments beneath Breidamerkursandur and the form of the underlying bedrock in Sigbjarnarson (ed) Iceland Coastal and River Symposium: Proceedings Reykjavik, Iceland.

Bjørnsson H, 1996. Scales and rates of glacial sediment removal: a 20 km long, 300 m deep trench created beneath Breidamerkurjökull during the Little Ice Age.
Annuals of Glaciology, 22, 141–146.

Boulton G S, Caban P, Hulton N, 1999. Simulation of the Scandinavian ice sheet and its sub-surface conditions.
SKB R-99-73, Stockholm.

Boulton G S, Caban P E, van Gijssel K, 1995a. Groundwater flow beneath ice sheets: Part I – Large scale patterns.
Quaternary Science Reviews, Vol 14, 545–562.

Boulton G S, Caban P E, Punkari M, 1995b. Sub-surface conditions in Sweden produced by climate change, including glaciation. Project 2 – Sensitivity tests and model testing.
SKB Arbetsrapport 95-42, Stockholm.

Boulton G S, Caban P E, 1995. Groundwater flow beneath ice sheets: Part II – Its impact on glacier tectonic structures and moraine formation.
Quaternary Science Reviews, Vol 14, 563–587.

Boulton G S, Hindmarsh R C A, 1987. Deformation of subglacial sediments: rheology and geological consequences.
J Geophys Res, 92, 9059–82.

Boulton G S, Payne A, 1994. Northern hemisphere ice sheets through the last glacial cycle: glaciological and geological reconstructions. In Duplessy J-C and Spyridakis M-T, eds. Long term climatic variations: data and modelling. NATO ASI Series 1 – Global Environmental Change.
Springer-Verlag, Stuttgart, 177–212.

Boulton G S, Hindmarsh R C A, 1987. Sediment deformation beneath glaciers: rheology and geological consequences.
J Geophys Res, 92(B9), 9059–9082.

Clark P U, Walder J S, 1994. Subglacial drainage, eskers, and deforming beds beneath the Laurentide and Eurasian ice sheets.
Geol Soc Am Bull, 106, 304–314.

De Geer G, 1897. Om rullstensasarnas bilmingssatt.
Geologiska Foreningens i Stockholm, Forhandlingar 19, 366–388.

Engelhardt H, Harrison W D, Kamb B, 1978. Basal sliding and conditions at the glacier bed as revealed by borehole photography.
Journal of Glaciology, 20, 469–508.

Fountain A G, 1994. Borehole water-level variations and implications for the subglacial hydraulics of South Cascade Glacier, Washington State.
J Glaciol, 40, 293–304.

Hallet B, Anderson R S, 1980. Detailed glacial geomorphology of a proglacial bedrock-area at Castleguard Glacier, Alberta, Canada.
Zeitschrift fur Gletscherkunde und Glazialgeologie 16, 171–184

Hantz D, Lliboutry L, 1983. Waterways, ice permeability at depth and water pressures at the Glacier d'Argentière, French Alps.
Journal of Glaciology, 29, 227–239.

Hubbard B P, Sharp M J, Willis I C, Nielson M K, Smart C C, 1995. Borehole water-level variations and the structure of the subglacial hydrological system of Haut Glacier d'Arolla, Valais, Switzerland.
Journal of Glaciology 41, 572–583.

Hughes T, 1975. The West Antarctic Ice Sheet: instability, disintegration and initiation of ice ages.
Reviews of Geophysics and Space Physics, 13, 502–526.

Huybrechts P, 1986. A three-dimensional time-dependent numerical model for polar ice sheets: some basic testing with a stable and efficient finite difference scheme.
Report 86-1, Vrije Universiteit, Belgium.

Kamb B, 1987. Glacier surge mechanism based on linked cavity configuration of the basal water conduit system.
J Geophys. Res, 92 (B9), 9083–9100.

Lliboutry L, 1968. General theory of subglacial cavitation and sliding of temperate glaciers.
J Glaciol, 7, 21–58.

Lundquist J, 1996. Professor emeritus Stockholm University.

Maillot B, Main I G, 1996. A lattice BGK model for the diffusion of pore fluid pressure including anisotropy, heterogeneity, and gravity effects.
Geophys Res Lett, 23, 1, 13–16.

Morland L W, Boulton G S, 1975. Stress in an elastic hump: the effects of glacier flow over elastic bedrock.
Proc R Soc Lond A 34, 157–173.

Nye J F, 1973. Water at the bed of a glacier, IAHS Publ, 95, 189–194.

Paterson W S B, 1994. The Physics of Glaciers. 3rd Edition. Pergamon

Piotrowski J A, 1994. Tunnel valley formation in north-west Germany: geology, mechanisms of formation and subglacial bed conditions for the Bornhoved tunnel valley. Sedimentary Geology 89, 107–141.

Praeg, 1996. Morphology, stratigraphy and genesis of buried mid-Pleistocene Tunnel-Valleys in the southern North Sea Basin. Unpublished Phd thesis.
University of Edinburgh.

Reynaud L, 1989. Crevasses, seracs, moulins et cavites sous glaciaires. Neiges et Avalanches.
Revue de l'ANENA, 49, 8–13.

Röthlisberger H, 1972. Water pressure in intra- and subglacial channels.
J Glaciol, 11, 177–203.

Shreve R L, 1972. The movement of water in glaciers.
Journal of Glaciology, 11, 205–214.

Shreve R L, 1985. Esker characteristics in terms of glacier physics, Katahdin esker system, Maine.
Geol Soc Am Bull, 96, 639–646.

Van Weert F H A, Leijnse A, 1996. Modelling the effects of Pleistocene glaciations on the Northwest European geohydrological situations.
Rijksinstituut voor Volksgezondheid en Milieu, Report 715401001.

Walder J S, 1982. Stability of sheet flow of water beneath temperate glaciers and implications for glacier surging.
J Glaciol, 28 (99), 273–293.

Walder J S, Fowler A, 1994. Channelized subglacial drainage over a deformable bed.
Journal of Glaciology 40, 3–15.

Weertman J, 1972. General theory of water flow at the base of a glacier or ice sheet.
Rev Geophys Space Phys, 10 (1), 287–333.

Willis I C, Sharp M J, Richards K S, 1990. Configuration of the drainage system of Mitdalsbreen, Norway, as indicated by dye-tracing experiments.
Journal Glaciology 36, 89–101.

Woodworth J B, 1899. The ice-contact in the classification of glacial deposits.
Am Geologist, 23, 80–86.

White F M, 1979. Fluid Mechanics, McGraw-Hill, Inc. Tokyo

Observations of groundwater and tunnel flow in a modern glacier

1 The field experiment

A drilling and monitoring programme was undertaken during August 1989 until March 1990 on the glacier Breidamerkurjøkull in S.E. Iceland in order to explore relationships between tunnel flow and groundwater flow. Breidamerkurjøkull is a southern outlet glacier of the ice cap Vatnajøkull. It has a length of 30 km, from the Vatnajøkull ice divide to its ice margin, which has a width of 15 km. The glacier is dissimilar to the many valley glaciers whose hydrology has been studied which have irregular rock beds, but its bed is similar to the unlithified sediment beds, which underlay large areas of midlatitude ice sheets. In its outer 12 km it overlies a flat plain /Bjørnsson, 1996/ formed of a thick sequence of unlithified sediments /Boulton and others, 1982/ which, in the terminal area of the glacier, comprise up to 50 m of fluvioglacial gravels and tills overlying fractured volcanic rocks /Bogadottir and others, 1985/.

An experimental area was chosen on the west side of the glacier, in the vicinity of the point of discharge of a major subglacial stream at the glacier margin, see Figure 1-1. A borehole, drilled using a rotary technique, near to the glacier margin at D1, penetrated some 28 meters of sandy sediment (no core was retrieved). No further penetration was

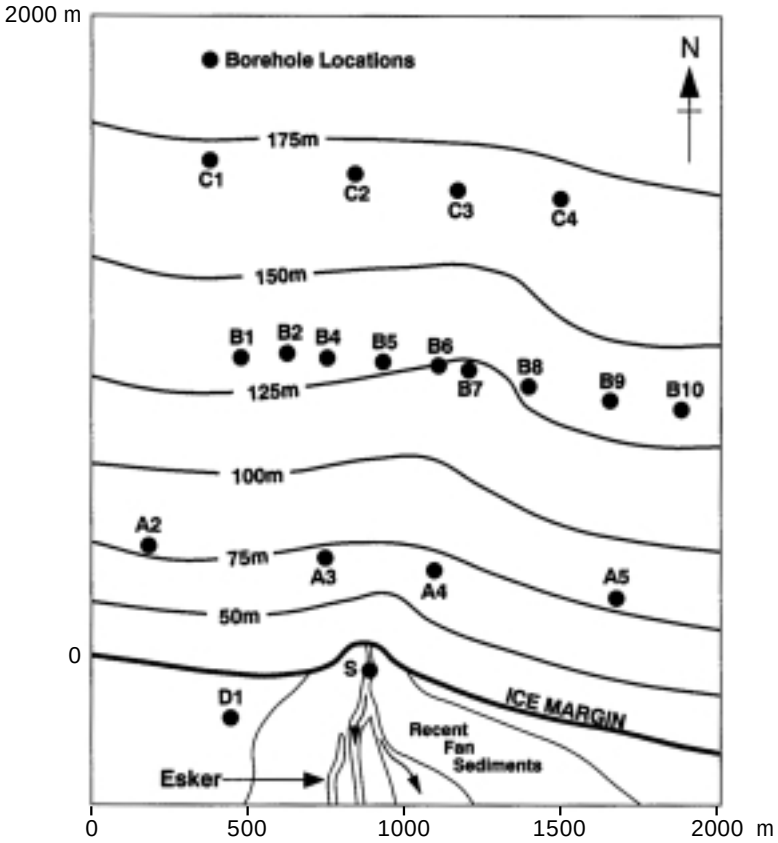

Figure 1-1. *The experimental area at Breidamerkurjökull showing the locations of boreholes.*

possible because of a resistant rock mass, which may have been a large boulder or bedrock. Seismic sounding in the area /Bogadottir and others, 1985/ suggested that bedrock lay at a depth of between 0.3 and 50 m. A series of pumping tests over 24 hour periods were undertaken through slotted casing using packers which permitted predetermined sections of the borehole to be tested.

As a guide to drilling on the glacier, a radio-echo survey was undertaken of an area extending 2 km from the glacier margin and 2 km in cross-glacier extent (Figure 1-1). It revealed a subglacial valley extending northwards from the stream portal, which we assume to indicate the location of the subglacial stream. Using this survey as a guide, a further series of boreholes were drilled through the glacier (Figure 1-1), using a 20 cm diameter thermal drill to penetrate within a few metres of the glacier sole, and a rotary drill system to penetrate through the basal ice and into the bed. Rotary drilling through the basal ice and into the sediment column used casing with a hardened drilling crown. The maximum penetration into the bed was 11 m. Six drill holes were abandoned before the glacier sole had been reached. Down-hole photographs suggested that this tended to occur because of debris layers in the ice, which clogged the drill bit and slowed down drilling excessively. Pore-fluid pressures were measured in four boreholes by piezometers in sections isolated by packers. In other boreholes, porewater pressure variation was measured by fluctuations of the water surface in the borehole as registered by conductivity metres. All boreholes were completed within one to two days and monitored continually until the end of the experimental period, unless there was evidence that connection to the subglacial environment had been severed. This was normally assumed to be when diurnal pressure fluctuations in the borehole ceased. The most complete records were obtained from a period after completion of drilling on 28 September until 16 October when the first borehole ceased to monitor bed fluctuations. Monitoring at boreholes C1–C4 ceased by the end of October, boreholes A2–A5 had ceased monitoring by the end of December, and of the boreholes in transect B, B6–B7 continued well into the new year and B7 continued until 27 February.

2 Results and interpretation

Figure 2-1 shows a transverse transect across the glacier surface about one km from the ice margin and across the line of subglacial stream valley. It shows two hour (12.00–14.00 hr) average piezometric surfaces reconstructed from operational boreholes on 28 September, 6 October, 11 November, 13 December and 20 December. Borehole B4 penetrated 5.2 m into sandy silt subglacial sediment and B7 penetrated 4.6 m into silt rich sediment. Both are believed to have directly measured the natural groundwater head.

The low points in the piezometric surfaces shown in the Figure 2-1 transect coincide with the subglacial valley. We assume that this low point reflects the drawdown of groundwater heads by a subglacial stream, which passes through this low point. The general form of the piezometric surface and groundwater flowlines can be reconstructed with reasonable confidence. Figure 2-2 shows the average form of the surface and inferred flowlines between 1,200 and 1,400 hours on 7 October. It defines part of a groundwater catchment for the subglacial stream, a drainage divide for which probably occurs near the eastern extremity of transect B, where the groundwater head falls off towards the east between boreholes B8 and B10. The stream clearly occupies a subglacial valley, and emerges from beneath the glacier at the major stream portal at the ice margin. Using the interpolated contours in Figure 2-2, the maximum drawdown between the stream and the groundwater divide is at least 75–80 m. If we assume that similar patterns of drawdown are associated with all the major streams, which emerge from the margin of Breidamerkurjøkull, typical widths of groundwater catchments in the terminal zone of the glacier are 0.5 to 2 km.

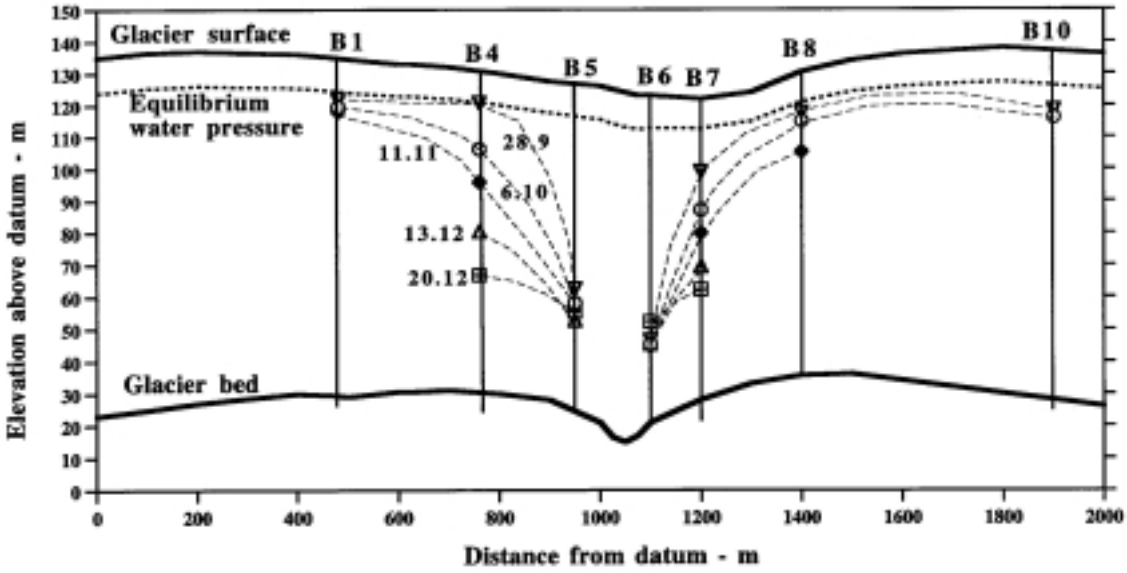

Figure 2-1. *Two-hour (12.00–14.00) average piezometric surfaces measured in boreholes B1–B10 on 28 September (28.9), 6 October (1.10), 11 November (11.11), 13 December (13.12) and 20 December (20.12).*

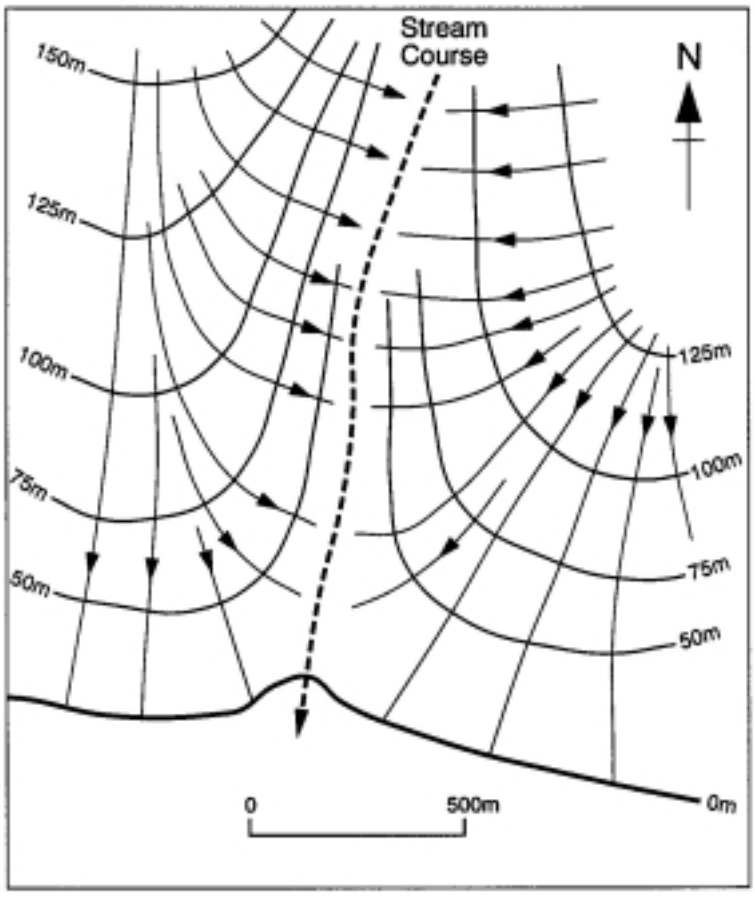

Figure 2-2. *Average form of the piezometric surface at the 28 September and inferred groundwater flowlines.*

Figure 2-3a shows water pressures in boreholes B1, B4 and B5, during the transition from autumn to winter. Heads show strong variability, which correlates with patterns of discharge from the subglacial stream portal (Figure 2-3b). This in turn correlates with measured patterns of rainfall and melting on the glacier surface in the terminal zone, see Figure 2-3c. We suggest that when surface water production is large, it penetrates to the bed through crevasses and moulins in the terminal zone, drives up groundwater heads, and is transported as groundwater into the subglacial tunnel, from which it is rapidly transported to the glacier margin by the subglacial stream. During the period 30 September–6 October, we estimate that about 40% of the surface melt and rainfall in the presumed area of the subglacial stream catchment, most of which was produced in the lowermost 5 km of the glacier, was discharged through the subglacial stream. From mid-November on, however, there are increasingly long periods of cold weather during which there is neither rainfall nor melting on the glacier surface. As we shall show in a subsequent article, transit times of surface meltwater through the glacier system are a maximum of 24–36 hours. Thus, the piezometric surface for 20 December, see Figure 2-1, 10 days after the last melt/rainfall event, must represent discharge of water derived from basal melting. This is compatible with rates of melting calculated from measurements and inferences velocity and shear stress in this zone, and inferred transmissivity magnitudes.

The groundwater heads shown in Figure 2-2 were selected to illustrate the overall fall in borehole heads during the transition from summer to winter seasons, although as Figure I.4a shows, periods of melting or rainfall in early winter drive up heads for short periods.

Temporal variations in head are relatively small to the subglacial stream (BH5, Figure 2-3a), presumably because they are strongly controlled by the pressure in the stream which must be relatively constant. They vary much more in boreholes furthest from the assumed subglacial stream. During periods of strong melting in summer and autumn, pressures in boreholes B1–B4 and B8–B10, near to presumed drainage divides, rise rapidly to within 5–10 m of a level where they equal the ice pressure, and approximately stabilise at that level. Only occasionally do water over-pressures occur.

We suggest that when heads lie well below the level of the ice pressure, subglacial water discharge into the stream takes place entirely by groundwater flow. When water pressure rise is large enough to produce effective pressures below the limiting value for shear deformation of subglacial sediments /Boulton and Hindmarsh, 1987/ dilation of these sediments and the formation of features such as “canals” /Walder and Fowler, 1994/ permits more effective drainage to take place near the ice/bed interface, such that further water pressure build up is inhibited, and the limiting pressure plateaux shown in Figure 2-3a (B1) develop.

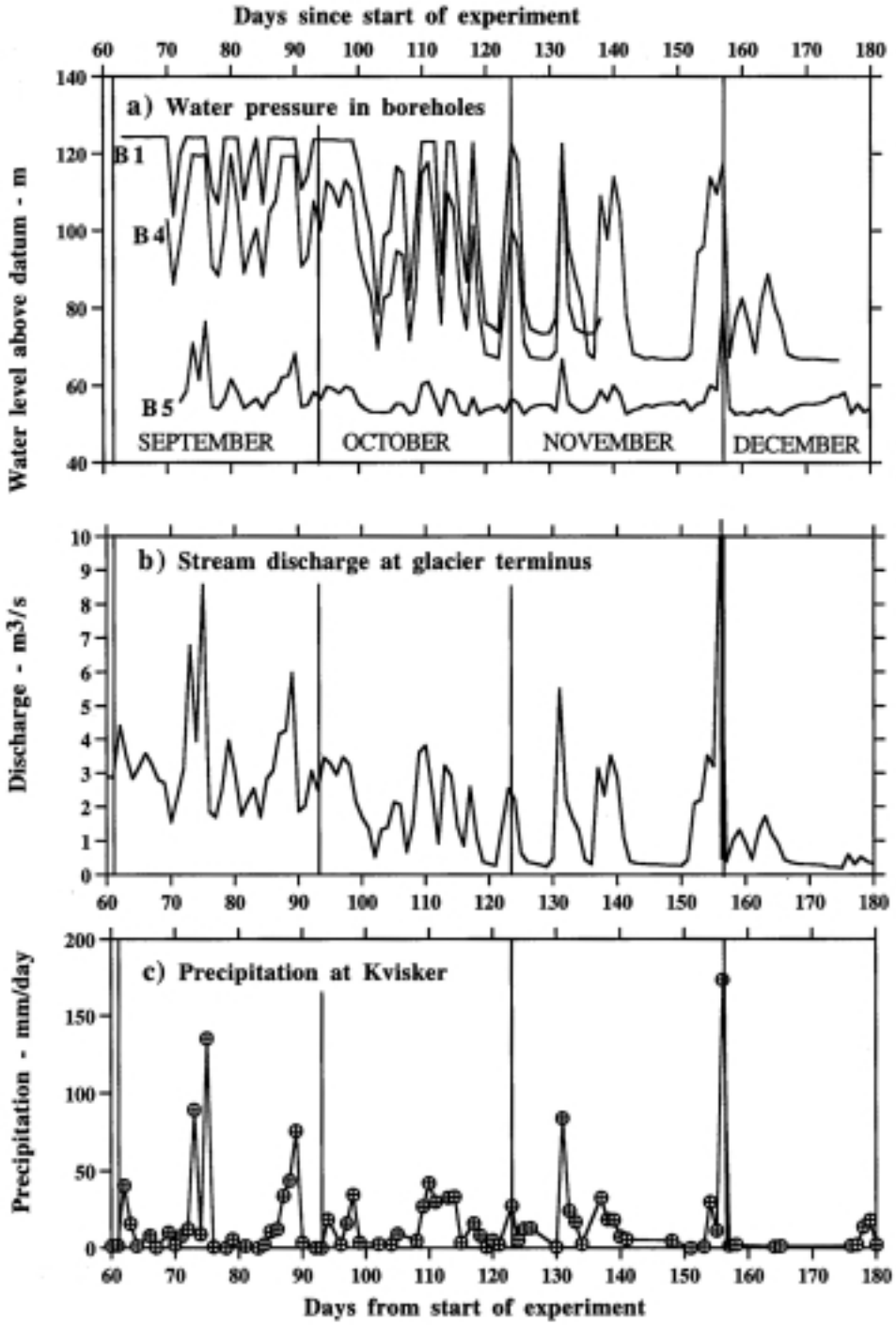

Figure 2-3.
a) *Water pressures in selected boreholes.*
b) *Stream discharge.*
c) *Precipitation at a nearby site for the experimental period.*

3 Eskers at Breidamerkurjøkull as evidence of subglacial tunnels

An esker lies just beyond the stream portal (Figure 1-1). It is a ridge, about 4 m in height, about 20 m wide at the base and of pyramidal cross-section. It is composed of coarse bouldery gravel, with some boulders up to 0.4 m in diameter. It is one of a series of discontinuous, co-linear ridges which extend from the stream portal as far as the Neoglacial maximum position of glacier in about 1890, some 4 km away. We suggest that the co-linear esker system faithfully records the successive positions the portal of the ancestors of the subglacial stream shown in Figure 2-2 as the ice margin has retreated during the last 100 year.

Eskers occur beyond the portals of all the major subglacial streams which drain to terrestrial margins of Breidamerkurjøkull, and are parts of systems which extend to the Neoglacial maximum position of the glacier. This suggests that the axes of the major subglacial streams have been stable for at least 100 years. Assuming that they all have relationships to the groundwater table of the nature shown in Figure 2-2, we suggest that their spacing, which are, on average, 2–3 km, also define groundwater divide spacings and catchments.

We have observed over several years that, as stream discharges fall during early winter, the subglacial tunnel may become partly blocked within the portal by bouldery sediment which the stream no longer has a capacity to transport, and that the lower, winter discharges are sometimes diverted around this sediment mass. High discharges during the next summer may either remove this deposited mass or be permanently diverted by it. This latter process seems likely to the one, which creates new esker segments, which are essentially part of a complex co-linear system.

Between the major esker systems there are commonly found small (>1 m) disconnected esker fragments, often composed of relatively fine grained materials, or shallow tunnels which appear to have formed subglacially. We suggest that these features formed during summer periods of strong glacier melting, when surface water draining to the bed in the terminal zone drives up water pressures in broad groundwater divide regions, so that small channels, pipes or canals are temporarily created. They are however poorly integrated, have high water pressures, low flow velocities, and have a relatively low sediment transporting. They cease to operate as discharges fall and do not re-form at the same sites in succeeding summers.

Solution of differential equation

The first-order non-linear differential equation for water pressure distribution along the tunnel:

$$\frac{dp_t}{dx} \quad BQ_0^{\ 2/11} q(x)^{\ 2/11} (p_i \quad p_t)^{8n/11} \tag{1}$$

has an analytical solution in the region of moderate water pressures $p_t = 1/2 p_i$. In this approximation Equation (1) reduces to the linear differential equation:

$$\frac{dp_t}{dx} = BQ_0^{-2/11} q(x) \left(p_i(x)^{8n/11} - \frac{8n}{11} p_t p_i(x)^{8n/(11-1)} \right) \tag{2}$$

It is convenient to introduce a new coordinate y along the tunnel:

$$y = BQ_0^{-2/11} \int_0^x q(x)dx \tag{3}$$

Equation (2) for water pressure as a function of y now reads:

$$\frac{dp_t}{dy} \quad \frac{8n}{11} p_t p_i(y)^{8n/11} \quad p_i(y)^{8n/11} \tag{4}$$

The differential Equation (4) has an integrating factor:

$$(y) = \exp\left\{ \frac{8n}{11} \int p_i(y)^{\frac{8n}{11}-1} dy \right\} \tag{5}$$

and a general solution:

$$p_t(y) = \frac{1}{(y)} \left((y_0) y_0 + \int_{y_0}^{y} (y') p_i(y')^{8n/11} dy' \right) \tag{6}$$

where y as a function of x is given by Equation (3).